

# **Land transformation across agroecological zones reveals expanding cropland and settlement at the expense of tree-cover and wetland areas in Nigeria**

\*Felicia O. Akinyemi<sup>1,2a</sup>, Chinwe Ifejika Speranza<sup>1b</sup>

<sup>1</sup>Land Systems and Sustainable Land Management, Institute of Geography, University of Bern, Hallerstrasse 12, 3012 Bern, Switzerland

<sup>2</sup>Geomatics, Department of Environmental and Life Sciences, Karlstad University, Universitetsgatan 2, 651 88 Karlstad, Sweden

<sup>a</sup>felicia.akinyemi@unibe.ch, akinyemi.felicia@gmail.com, <sup>b</sup>chinwe.ifejika.speranza@unibe.ch

*This paper is a non-peer reviewed preprint submitted to EarthArXiv. It has been submitted to the Geo-Spatial Information Science for peer review*

---

<sup>1</sup> \*Corresponding author. Land Systems and Sustainable Land Management, Institute of Geography, University of Bern, Hallerstrasse 12, 3012 Bern, Switzerland, akinyemi.felicia@gmail.com +41 779693968

## Abstract

Evaluating how land-cover is being transformed is essential to identify patterns necessary to infer the change trajectories and the driving factors. This study considers the case of Nigeria, where various natural ecosystems are being converted and for which a current national scale assessment is lacking. Producing Landsat-based time-series, we analyze change among land-cover types (i.e., tree-covered area, grassland, wetland, waterbody, cropland, artificial surfaces and otherland) across seven agroecological zones. The annual intensity of change was assessed at multi-levels across two time-intervals (i.e., 2000 – 2013, 2013 – 2022). Distinguishing between natural land-cover and human activity-related land-use, we estimate the extent of change signifying how humans have appropriated natural land-cover. Insights from analysis at the interval level reveal that land transformation accelerated from 3.3% in 2000 – 2013 to 4.5% during 2013 – 2022 in all agroecological zones (e.g., rainforest, mangrove), except in Sudan and Sahel savannah where speed was higher in 2000 – 2013 as grasslands were increasingly cultivated. Cropland expanded almost two-fold (22% to 37%), whereas tree-cover declined from 50% to 31% and wetland from 7% to 3.7% over the 23 years. Much loss of natural land-cover (e.g., tree-cover, grassland and wetland) to cropland mainly occurred in 2000 – 2013 (22%) when most irrigation schemes in Nigeria were established. In contrast, the loss of natural land-cover to settlement (0.9%) during 2000 – 2013 increased to 2.0% in 2013 – 2022. Of all agroecological zones, the mangrove zone was most disturbed as its persisting land-cover areas reduced from 69% to 5% between 2000 – 2013 and 2013 – 2022. The amount of persisting land-cover was highest in the Sudan Savannah at 44% in 2000 – 2013 and 49% in 2013 – 2022. Processes of human appropriated natural land-cover in Nigeria are related to urbanization and cropland expansion into natural areas with some instances of natural regeneration, especially in abandoned croplands and settlement areas.

*Key words:* Land cover, Agroecological zone, Intensity, Human-appropriated natural land-cover, Random Forest

### *Highlights*

- The speed of LULC change (annual rates) accelerated from 3.3% yr<sup>-1</sup> in 2000 – 2013 to 4.5% yr<sup>-1</sup> in 2013 – 2022 in all agroecological zones (e.g., rainforest, mangrove), except in the semi-arid Sudan and Sahel savannah where speed was higher in 2000 – 2013 due to the cultivation of grasslands made possible by irrigation.
- Main change processes in Nigeria (2000 – 2022) are primarily related to the dominance of human activities as more natural cover was lost to cropland and artificialisation, e.g., settlement development than was gained for nature, e.g., through natural regeneration and afforestation, during all time intervals. For example, the loss of natural land cover to settlement increased from 0.9% to 2.0% between 2000 – 2013 and 2013 – 2022.
- Agriculture, through converting natural cover to croplands, remains the major direct driver of land cover change in the last three decades.
- The natural regeneration and afforestation process contributed to driving changes to land cover during all two time-intervals.

## 1. Introduction

The toll on natural resources to provide food, feed, fibre, water, energy and shelter for more than seven billion people on the planet has never been so great. Converging evidence shows that humans increasingly appropriate natural land-cover (e.g., Alexander et al., 2016; Twongyirwe et al., 2018; Winkler et al., 2021; Wang et al., 2023). Current and timely information on changes to land-cover and land-use is essential to maintain ecosystem functions, prevent land resources from degrading, provide accurate carbon accounting, and take land-based climate action (Findell et al., 2017; Yue et al., 2020). With mounting human pressure on land-based natural resources, evaluating human-appropriated natural land-cover (HANLC) will inform use (UNCCD, 2019; Herrmann et al., 2020; Akinyemi and Ifejika Speranza, 2022).

Knowledge is to be gained from a multiyear assessment of changes to land-cover. The case of Nigeria is examined as it is an agroecologically diverse context and a hotspot of land-cover change (FAO, 2020; Akinyemi and Ifejika Speranza, 2022). While changing land conditions in Nigeria need monitoring, land-cover time-series datasets are lacking. Although the time-series can be provided through Remote Sensing, the potential has not been fully utilized in this context (Ifejika Speranza et al., 2023). Most available products are often outdated and provide a one-time snapshot of land-cover for single periods which is inadequate to assess change. Nigeria's most recent national scale analysis of land-cover was only up to 2016 (FAO, 2020). Thus, knowledge of ongoing changes to land-cover at national and local levels is very limited.

A multi-level assessment of the annual intensity of land-cover change was conducted using two time-intervals (i.e., 2000–2013 and 2013–2022). We examined the intensity of change at the interval and category levels and by agroecological zones (AEZ). The interval level analysis provides the speed at which land was transformed during an interval and compares this across all time-intervals. In contrast, the change intensity for each category is computed in terms of its gross loss and gross gain during each time-interval (Aldwaik and Pontius, 2012). The AEZ level analysis calculates the intensity of land-cover change for each zone. The assumption of uniform agroecological conditions is inappropriate for a diverse context like Nigeria. Limiting further analysis to major change patterns exemplifying human appropriation of natural land-cover (HANLC), we estimated the extent of HANLC, identified the processes and drivers as well as outcomes along agroecological gradients for which little work has yet been done in Nigeria.

The objectives of this study are three. First, we produced land-cover data in Nigeria for three time points (i.e., 2000, 2013, 2022). Second, we conducted a multi-level assessment of the annual intensity of land-cover change during 2000 – 2013 and 2013 – 2022 across seven AEZs. Third, we estimated the extent of change in HANLC areas resulting in the loss of natural land-cover such as in tree-covered areas, wetlands and grasslands. The following subsections describe the methods

used to create the land-cover datasets and quantify the annual intensity of change across time-intervals. We present the results of the multi-level analyses of change intensity during each time-interval and how this differed between categories in AEZs. Further, we present and discuss the drivers and processes of HANLC changes. This study contributes to efforts to monitor anthropogenic-induced land-cover changes in predominantly tropical forest-agriculture mosaic landscapes.

## **2. MATERIALS AND METHODS**

### **2.1. Study area**

Nigeria has a land area of approximately 910,731 km<sup>2</sup>. With an estimated 223,804,632 million inhabitants (2.8% of the world's population), it is the most populous African country (Department of Drought and Desertification Amelioration, 2018; UNFPA, 2023). It is bordered in the south by the Atlantic Ocean and has Niger, Benin, Cameroon and Chad as neighbors (Fig. 1). Nigeria stretches across multiple latitudes with diverse agroecological conditions (Fig. 1a) and elevations (Fig. 1b). Agroecological conditions range from the ultra humid in the mangrove, freshwater swamps — FWS and Rainforests — RaF (>2000mm yr<sup>-1</sup> rainfall and monthly temperature (tmin/tmax) of 23 – 33°C), sub-humid in the Guinea Savannah — GS (>1000mm yr<sup>-1</sup> rainfall and 20 – 37°C tmin/tmax) to the Sudan Savannah — SS and Sahel Savannah — SaS (440 – 600mm yr<sup>-1</sup> rainfall and 13 – 40°C tmin/tmax) (Iloeje, 2001; Adelodun and Choi, 2018). Lake Chad, in the country's northeast, is a Ramsar site differentiated from the SaS due to its lacustrine context. In most regions, the rainy season is from March/April to October, with the southern part having bimodal rainfall distribution, whereas the dry season (Harmattan) is from November to March.

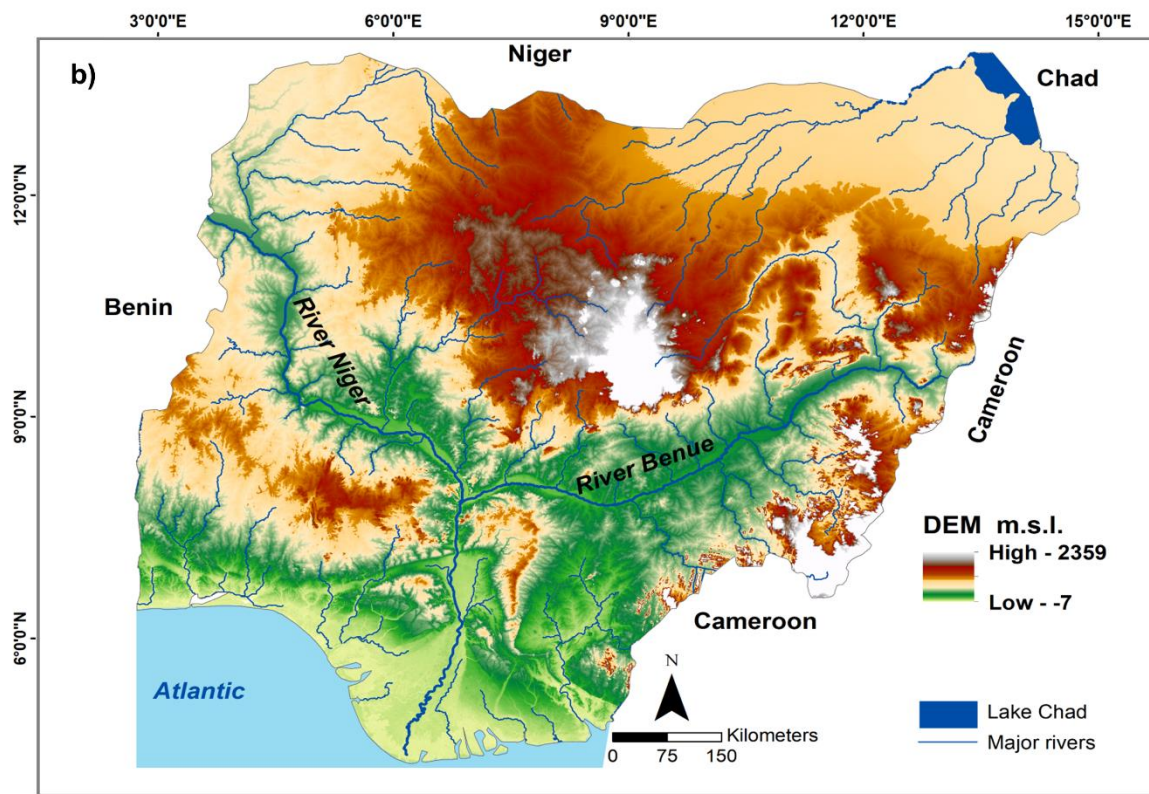
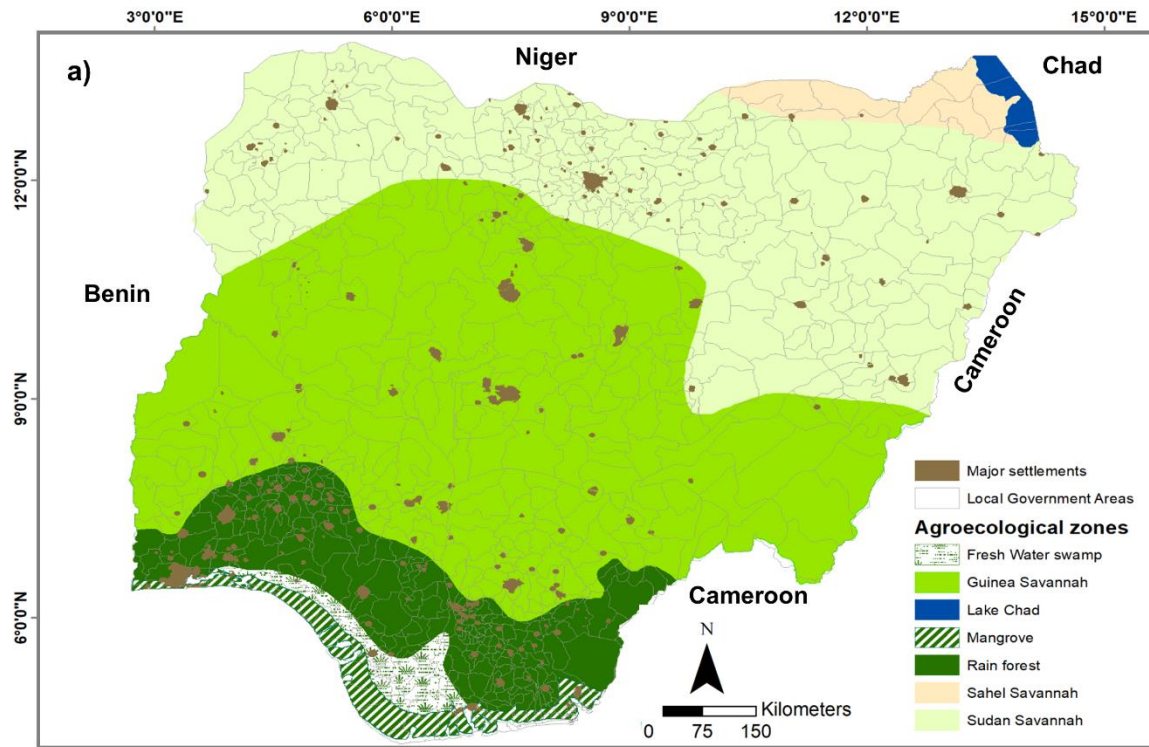


Figure 1. Nigeria, a) Agroecological zones, major settlements and Local Government Areas (3<sup>rd</sup> administrative level), b) Biophysical map depicting elevation, topography, major rivers and lakes.

## 2.2. Workflow

The steps in the workflow, depicted in Fig. 2, are a) Data collection and preprocessing, b) Image classification and change detection, c) Multi-level assessment of the intensity of land-cover change, and d) Evaluating HANLC changes. From high-resolution images, reference data were collected on the field and in Google Earth Pro (GEP). Preprocessing and classification were conducted in Google Earth Engine (GEE), and postprocessing was done in QGIS/ArcGIS.

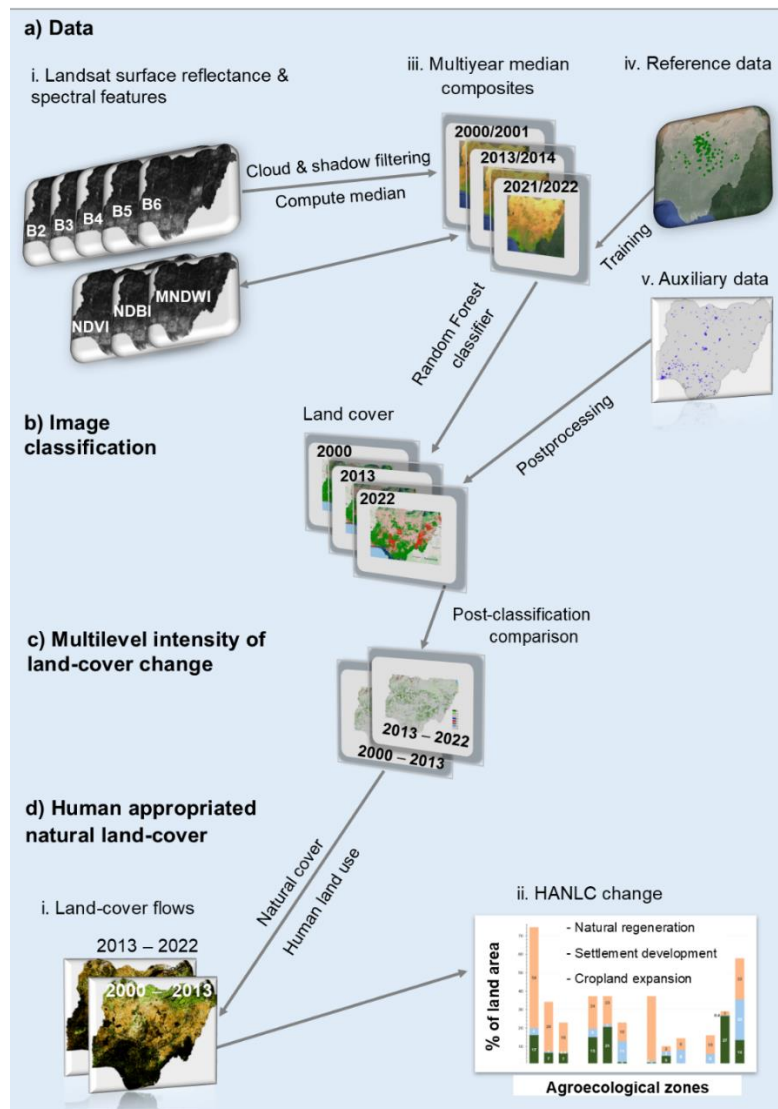


Figure 2. Workflow used for analyses. **a) Input data**, i-ii. Preprocessing of images and multiyear composites — Surface reflectance median bands, Normalized Difference Vegetation Index (NDVI), Modified Normalized Difference Water Index (MNDWI), Normalized Difference Built-up Index (NDBI), iii. Reference datasets used for training and validation iv. Auxiliary data for postprocessing land-cover maps for misclassified settlements and wetlands **b) Image classification** of land-cover with Random Forest classifier for 2000, 2013, 2022 **c) Intensities of land-cover change** computed at the interval and category levels for 2000 – 2013, 2013 – 2022 **d) Human-appropriated natural land-cover (HANLC)**, i. Land-cover flows between natural land-cover and human activity-related land-uses, ii. Estimates of HANLC changes by agroecological zones.

## 2.3 Data collection and image preprocessing

The multi-level assessments of annual change intensity and HANLC were conducted using datasets of the highest quality selected based on availability. Datasets used are satellite remote sensing images, reference data needed for image classification and validation, and other datasets such as the Nigerian boundary used to constrain analyses to the study area. Table 1 provides details of these datasets.

Table 1: Datasets used in this study

Dimension	Indicator	Unit/year	Data	Remark
Satellite images	Land-cover mapping and change detection	30m 2000, 2001, 2013, 2014, 2021, 2022	Landsat 7, 8 Surface reflectance Tier 1, level 2	<a href="https://www.usgs.gov/landsat-missions/landsat-collection-2-surface-reflectance">https://www.usgs.gov/landsat-missions/landsat-collection-2-surface-reflectance</a>
	Stratified random samples of seven land-cover categories	2022 2000, 2013, 2022	Field-based High-resolution images	July-November 2022 Google Earth Pro
Reference datasets	Land-cover	2km 2000 and 2013	USGS land-use maps	<a href="https://pubs.er.usgs.gov/publication/fs20173004">https://pubs.er.usgs.gov/publication/fs20173004</a>
	Elevation	1996 30 arc-second	Digital Elevation Model of Africa USGS	Center for Earth Resources Observation and Science <a href="https://databasin.org/datasets/2965da954b114ff3b47621e99e3b29ba/">https://databasin.org/datasets/2965da954b114ff3b47621e99e3b29ba/</a>
Auxiliary	Agroecological zones	2001 Boundary		Iloeje, 2001
	Major rivers and lakes	2014, 2015	FAO rivers RCMRD water bodies in Africa	FAO rivers in Africa, <a href="http://geoportal.rcmrd.org/layers/servir%3Aafrica_water_bodies">http://geoportal.rcmrd.org/layers/servir%3Aafrica_water_bodies</a>
	Nigerian boundary	Administrative boundary	Common Operational Database	UN Office for the Coordination of Humanitarian Affairs
	Built-up surface	2000, 2015 and 2020	Global Human Settlement	Joint Research Centre (JRC-GHS), Pesaresi and Freire (2016)

### 2.3.1 Satellite data and preprocessing

The median of Landsat 7 (ETM+) and 8 (OLI) 30m surface reflectance tier 1 image bands (henceforth LSR) (Fig. 2ai) were used to create multiyear image composites for 2000, 2013 and 2022 (Fig. 2aii). Only LSR was used for comparability because it meets the geometric and

radiometric quality requirements for multitemporal and multispectral mapping of land-cover (USGS, 2021). It is spatially registered and atmospherically corrected, including orthorectification (Main-Knorn et al., 2017). Atmospheric correction involves calibrating raw digital numbers to Top of Atmosphere reflectance to account for solar elevation and seasonal variable Earth-Sun distance, which is then corrected to surface reflectance (Young et al., 2017). Surface reflectance images have reduced variability between multiple images of different dates over the same area (Pons et al., 2014). For further details about processing LSR images from various Landsat missions, including the algorithms used, see USGS (2023).

We filtered the LSR images for cloud and cloud shadows using mainly the Landsat QA\_PIXEL band and retained only images with <=70% cloud cover. After cloud filtering, some images had gaps as some pixels were without data, especially for the year 2000, whereas gaps were minimal in images of other years. Since single-date or monthly image composites were not optimal for use due to excessive cloud cover and cloud shadows in the coastal regions, these necessitated creating multiyear composites with images from the immediate previous and subsequent years. Afterwards, we computed the median of each LSR image band in the multiyear image composites. Three spectral features that are beneficial in capturing the biophysical conditions of the land surface were computed from the median bands as in Eqs. 1 – 3. These spectral features are the Normalized Difference Vegetation Index (NDVI), Modified Normalized Difference Water Index (MNDWI), and the Normalized Difference Built-up Index (NDBI). The MNDWI is especially useful for distinguishing surface water features often correlated with built-up areas in other spectral indices (Mack et al., 2017).

$$NDVI = \frac{\text{Near Infrared (NIR)} - \text{Red}}{\text{Near Infrared (NIR)} + \text{Red}} \dots \dots \dots 1)$$

$$MNDWI = \frac{\text{Green} - \text{Shortwave Infrared (SWIR)}}{\text{Green} + \text{Shortwave Infrared (SWIR)}} \dots \dots \dots 2)$$

$$NDBI = \frac{\text{Shortwave Infrared (SWIR)} - \text{Near Infrared (NIR)}}{\text{Shortwave Infrared (SWIR)} + \text{Near Infrared (NIR)}} \dots \dots \dots 3)$$

With the vast geographic size of Nigeria, preprocessing and classifying more than 2400 images per time point, as in this study, would have been very computationally demanding and time-consuming without access to the cloud computing platform.

### *2.3.2. Reference data*

We created 55 data samples per category for training and validating the classified maps (Fig. 2aiii). Using stratified sampling ensures sufficient samples of each class are produced and well-distributed (McRoberts, 2014). The seven strata are tree-covered areas, grassland, cropland, wetland, artificial surfaces, otherland, and waterbody. Fieldwork was conducted in 2022 (July – November) and more data samples were collected from high-resolution images in GEP. For 2000 and 2013, reference datasets were independently generated in GEP and from the USGS land-use maps (USGS-WA) of 2000 and 2013, respectively (Tappan et al., 2016). USGS-WA, comprising 26 categories for West Africa, was validated by national partners (Cushing et al., 2016; Cotillon and Mathis, 2017). Sampling points generated from USGS-WA were cross-checked for correctness using images in GEP. This latter step forestalled the potential transfer of errors from existing maps to the samples generated. Some studies utilizing USGS-WA maps are Herrmann et al. (2020) and Barnieh et al. (2022).

### *2.3.3. Ancillary data*

AEZ boundaries were used as mapping units for analyzing land-cover change intensity. The outline of fragmented and cultivated wetlands (e.g., Hadejia-Nguru, Lake Chad) were digitized in GEP for year 2000, 2013 and 2022. The JRC built-up surface datasets for 2000, 2015 and 2020 were used to create settlement masks as binary maps for each time point in ArcGIS for use in postprocessing the land-cover maps (Fig. 2aiv).

## **2.4. Image classification**

For image classification, the median blue, green, red, NIR, and SWIR LSR bands and the three spectral features were used (Fig. 2ai).

### *2.4.1. Classification scheme*

We used the United Nations Convention to Combat Desertification (UNCCD) classification scheme comprising seven categories (Table 2). This scheme was used to support Nigeria's Land Degradation Neutrality (LDN) baseline setting (2000-2015) and monitoring till 2030 (Sims et al. 2021).

Table 2. The classification scheme used in this study

Code	Class name	Description	Photograph
1	Tree-covered area	Tree-covered area class is broader than the forest class as it comprises forests, savannahs, plantations, thickets and woodlands.	
2	Grassland	Grasses are dominant in this class with 0.3m to 2m grass height. It comprises steppe, Sahelian short grass and herbaceous savannah.	
3	Cropland	Cultivated land used for growing. Land is cleared with little or no vegetation cover.	
4	Wetland	Wetland comprises inundated and gallery vegetation. These fragile ecosystems occur on alluvial plains and marshes (e.g., the freshwater swamps and mangroves in the southern coastal areas).	
5	Artificial surface areas (settlement, roads infrastructure)	The category comprises ~80–100% of buildings constructed with concrete, mud or other materials. Spectral reflectance from rooftops depends mainly on the material used (e.g., corrugated sheets or ceramic roof tiles).	
6	Otherland	This category comprises exposed land surfaces with no or very little vegetation (e.g., barelands, exposed rock outcrops, sandy areas, open mines and Bowe).	
7	Waterbody	Open water surfaces with >95% cover of water, e.g., Asejire dam, Rivers Niger and Benue, etc.	

#### 2.4.2. Land-cover mapping and accuracy assessment

Applying the Random Forest (RF) machine learning algorithm, we produced land-cover maps for 2000, 2013 and 2022 (Fig. 2b). RF is an ensemble method suitable for classifying categorical values as used in land-cover maps (Breiman, 2001; Pelletier et al., 2016). For the three time points for mapping land-cover, 300 trees were used with the nodes per split set as the square root of the total number of input variables (Akinyemi et al., 2021). As a decision tree-based method, RF is applied to massive datasets owing to its computational simplicity and robustness to handle noise

and overtraining. As a non-parametric, normality is not assumed (Löw et al., 2015) and is less dependent on strong *a priori* assumptions about a class's statistical properties (Canty, 2019; Schonlau & Zou, 2020).

We computed the overall accuracy (OA), user accuracy (UA) and producer accuracy (PA) to validate the land-cover maps produced. Wetlands were difficult to distinguish from croplands when cultivated or when the spectral reflectance from the inundated vegetation resembles the reflectance from other vegetation types. Classifying settlement pixels in rural areas in highly forested regions was also problematic. Class confusion necessitated relabeling misclassified pixels using the wetland and settlement binary masks created for postprocessing.

## 2.5 Multi-level assessment of the intensity of land-cover change

Land-cover maps of 2000, 2013 and 2022 were used as input for change detection during two time-intervals (i.e., 2000 – 2013 and 2013 – 2022). Applying the post-classification bi-temporal method, we derived a change matrix of transitions between categories using a per-pixel-based approach overlaying independently classified images of two time points (Young et al., 2017; Akinyemi, 2018). Change patterns between land-cover categories are to be detected for each time-interval to compute the multi-level annual intensity of observed changes. With the interval's initial time in the rows and the final time in the columns, the matrix expresses the land area under each category and quantifies land transitions between categories. A change budget that explicitly quantifies each category's persistence, gains and losses during the time-intervals is provided. The annual intensity of land-cover change was quantified (Fig. 2c) by time-interval and category levels as in Eqs. 4 – 6 (annotations in Table 3) (Aldwaik and Pontius, 2012).

Table 3: Mathematical notation for computing annual intensities of land-cover change patterns following Aldwaik and Pontius (2012).

Symbol	Description
$T$	number of time points (i.e., 2000, 2013 and 2022)
$t$	index for the initial time point of interval $[Y_t, Y_{t+1}]$ , where $t$ ranges from 1 to $T-1$
$Y_t$	year at the time point $t$
$n$	number of land-cover categories
$i$	index for a category at an interval's initial time point
$j$	index for a category at an interval's final time point
$C_{ij}$	proportion of the landscape that transitioned from category $i$ to category $j$ during interval $[Y_t, Y_{t+1}]$
$S_t$	annual change during interval $[Y_t, Y_{t+1}]$
$L_{ti}$	annual loss intensity of category $i$ during interval $[Y_t, Y_{t+1}]$ , relative to size of category $i$ at time $t$
$G_{tj}$	annual gain intensity of category $j$ during interval $[Y_t, Y_{t+1}]$ , relative to size of category $j$ at time $t+1$

The intensity of annual change ( $S_t$ ) during interval  $[Y_t, Y_{t+1}]$ , is computed as the size of change divided by the length of the time-interval and expressed as a percentage of the spatial extent. This provides the speed at which land was transformed during an interval (Akinyemi et al., 2017).

$$S_t = \frac{\text{change during } [Y_t, Y_{t+1}]}{(\text{length of } [Y_t, Y_{t+1}])(\text{extent size})} 100\% = \frac{\sum_{j=1}^n [(\sum_{i=1}^n C_{tij}) - C_{tjj}]}{(Y_{t+1} - Y_t)(\sum_{j=1}^n \sum_{i=1}^n C_{tij})} 100\% \dots \dots \dots 4)$$

Analyzing change between land-cover categories involves a gaining category and a losing category as the loss of one category is the gain of another category (Aldwaik and Pontius, 2013). Thus, loss at the category level ( $L_{ti}$ ) is computed as the observed intensity of the annual gross loss of the losing category  $i$  during interval  $[Y_t, Y_{t+1}]$  divided by the size of category  $i$  at the initial time point  $t$  (Eq. 5). In contrast, for gain ( $G_{tj}$ ), the annual gross gain of the gaining category  $j$  during interval  $[Y_t, Y_{t+1}]$  is divided by the size of category  $j$  at time  $t+1$  as in Eq. 6.

$$L_{ti} = \frac{\text{annual loss of } i \text{ during } [Y_t, Y_{t+1}]}{\text{size of } i \text{ at } Y_t} 100\% = \frac{[(\sum_{j=1}^n C_{tij}) - C_{tii}]/(Y_{t+1} - Y_t)}{\sum_{j=1}^n C_{tij}} 100\% \dots \dots \dots 5)$$

$$G_{tj} = \frac{\text{annual gain of } j \text{ during } [Y_t, Y_{t+1}]}{\text{size of } j \text{ at } Y_{t+1}} 100\% = \frac{[(\sum_{i=1}^n C_{tij}) - C_{tjj}]/(Y_{t+1} - Y_t)}{\sum_{i=1}^n C_{tij}} 100\% \dots \dots \dots 6)$$

Examining the intensity of annual change at these different levels is essential to gauge the speed at which land transformation occurred during an interval and how these varied between categories.

## 2.5 Evaluating human appropriation of natural land-cover

This study defines human-appropriated natural land-cover (HANLC) as the conversion of natural land-cover (NLC) into predominantly human activity-related land-use (HLU). This required differentiating between NLCs and HLU. Although NLCs are not entirely excluded from human use, NLCs were differentiated from HLU because they are not cultivated or developed. For example, although grasslands are subject to high grazing intensities, especially in SS and SaS, they were grouped as NLC since grasslands occur naturally in Nigeria (Jimoh et al., 2020).

Focusing on major processes of observed change patterns, transitions between land-cover categories were aggregated into HANLC classes for each time point (i.e., 2000, 2013, 2022). HANLC classes are: 1) Cropland expansion, 2) Settlement and infrastructure development (SID), and 3) Natural regeneration and afforestation (NRA) comprising areas of NLC recovery. The first and second classes are areas where HLU expanded into NLCs. We estimated the extent and changes of HANLC during both time-intervals. The latter formed the basis for identifying the drivers and processes underlying the observed HANLC changes across AEZ and at the national level (Fig. 2di-ii).

### 3. RESULTS

Against the backdrop of monitoring land transformation in Nigeria, maps of land-cover patterns (i.e., the spatial and temporal configuration) and changes over 23 years are presented. Beyond mapping land-cover change, this study measured the intensity of change patterns at multi-levels, including between land-cover categories and AEZs.

#### 3.1. Evaluating mapping accuracy

Accuracies with which the images were classified into seven land categories are summarized in Table 4.

Table 4: User, producer and overall accuracy for each category

Categories	Metric	2000	2013	2022
All categories	OA	76	93	84
Tree-covered areas	UA	63	96	59
	PA	85	89	87
Grassland	UA	70	76	89
	PA	62	90	47
Cropland	UA	63	72	78
	PA	48	82	77
Wetland	UA	87	93	100
	PA	100	96	100
Artificial Surfaces	UA	78	83	43
	PA	100	100	100
Otherland	UA	93	97	69
	PA	100	91	73
Waterbody	UA	99	99	100
	PA	87	98	92

Note: User accuracy (UA), Producer accuracy (PA), Overall accuracy (OA)

Compared to other categories, waterbody and otherland were well classified with high UA and PA values, except when otherland was confused with grassland, especially in 2022. Wetlands were mostly confused with croplands and sometimes tree-covered areas. For example, cultivated wetlands are difficult to distinguish from croplands. Wetland confusion with tree-covered area mainly occurred in riparian and flooded forests due to forest inundation. Artificial surfaces were not well captured in the classification, especially rural settlements occurring in agricultural and forested mosaic landscapes, because of their small size. See further details in Supplementary Information.

#### 3.2. Varying spatial configurations of land-cover

Land-cover configuration varied between 2000, 2013, 2022 (Fig. 3a, i-iii) and the dynamics during 2000 – 2013 and 2013 – 2022 (Fig. 3b i-ii). The amount of persistent land-cover and gains per

category from other categories were quantified. In 2022, cropland had the largest share of land (37%) of all seven categories, followed by tree-covered areas at 31%. This contrasts with the land-cover configurations of other years. Tree-covered areas declined from approximately 455,000km<sup>2</sup> in 2000, 357,000km<sup>2</sup> in 2013 to 285,000 km<sup>2</sup> in 2022 — the converted tree-covered area (170,000km<sup>2</sup>) corresponds to a size slightly larger than Tunisia (155,360km<sup>2</sup>). Cropland expanded from approximately 200,000km<sup>2</sup> in 2000, 284,000km<sup>2</sup> in 2013, to 333,000km<sup>2</sup> in 2022. Cropland in Nigeria grew by about 5700km<sup>2</sup> yr<sup>-1</sup> assuming a uniform annual amount of cropland gain over the 23-year study period — gained cropland area (131,000km<sup>2</sup>) corresponds to a size slightly larger than Greece (130,647km<sup>2</sup>). There was a steady increase in artificial surfaces from approximately 1.2% (10,500km<sup>2</sup>) in 2000, 2% (20,300km<sup>2</sup>) in 2013 to 3.7% (33,400km<sup>2</sup>) in 2022. Wetlands reduced from about 7% (63,600km<sup>2</sup>) in 2000, 3.4% (31,300km<sup>2</sup>) in 2013 to 3.7% (33,500km<sup>2</sup>) in 2022.

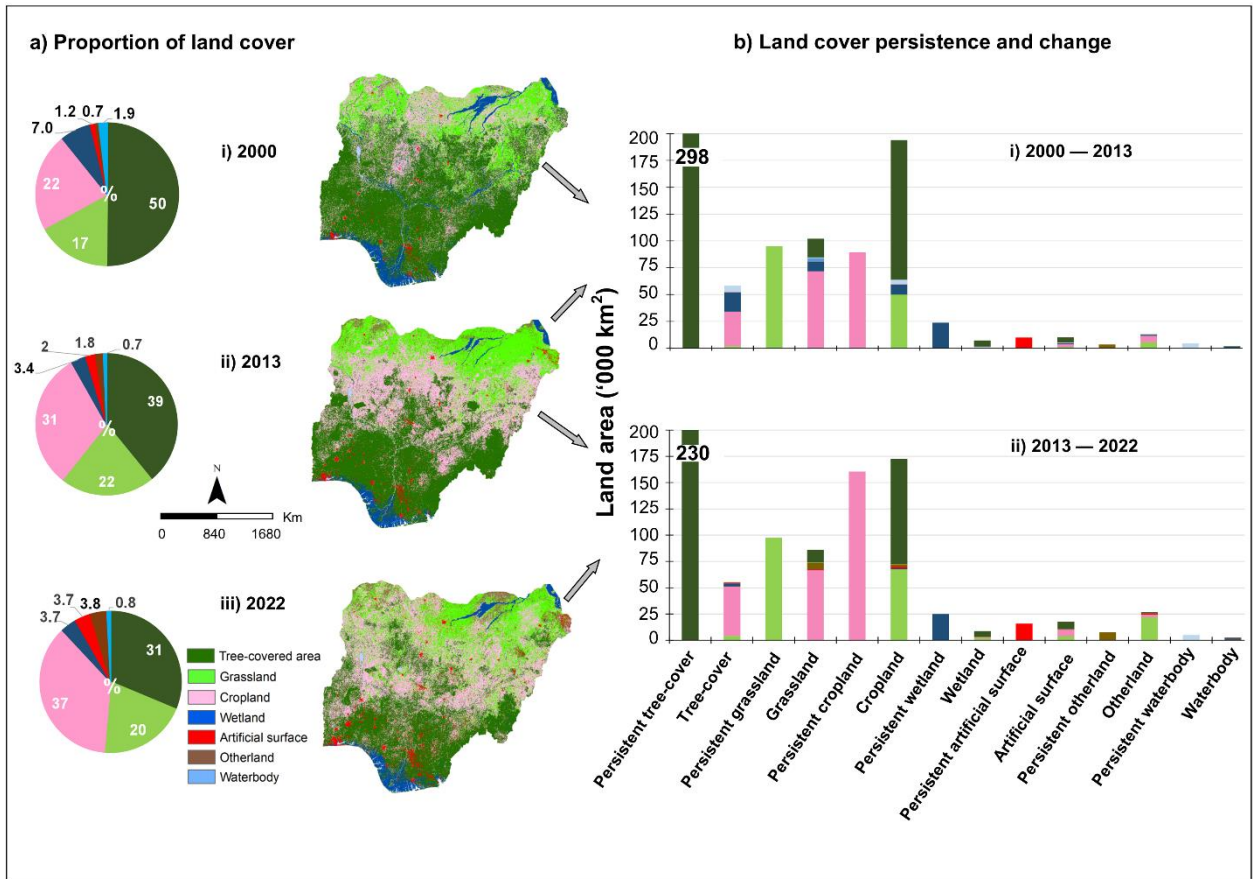


Figure 3. Land area of each category, a) Proportion of land per category (%) and the spatial distribution in ai. 2000, aii. 2013 and aiii. 2022. b) Amount of persisting land-cover and land gained by each category (km<sup>2</sup>) during the first time-interval (2000 – 2013) and second time-interval (2013 – 2022). Note that actual values of persistent tree-cover are depicted on the bars.

Fig. 3b (i-iii) shows persisting land-covers and areas where changes occurred during 2000 – 2013 and 2013 – 2022. Land area occupied by persisting land-covers was approximately 58% (524,000km<sup>2</sup>) in 2000 – 2013 and 59% (541,000km<sup>2</sup>) in 2013 – 2022. Most persisting are tree-covered areas, croplands and grasslands. Tree-covered area gained approximately 32,000km<sup>2</sup> and 18,000km<sup>2</sup> from cropland and wetland respectively in 2000 – 2013. In contrast during 2013 – 2022, tree-covered area gained approximately 47,000km<sup>2</sup> and 4,200km<sup>2</sup> from cropland and grassland respectively. During 2000 – 2013, grassland gained 72,000km<sup>2</sup> from cropland and 17,000km<sup>2</sup> from tree-covered area. In 2013 – 2022, grassland gains from cropland and tree-covered area were approximately 67,000km<sup>2</sup> and 12,000km<sup>2</sup> respectively. In 2000 – 2013, gains made by cropland were mostly from tree-covered areas (130,000km<sup>2</sup>) and grassland (50,000km<sup>2</sup>). In contrast during 2013 – 2022, cropland gains from tree-covered area and grassland reduced to 100,000km<sup>2</sup> and 67,000km<sup>2</sup> respectively. Otherland gained 2,425km<sup>2</sup> from croplands in 2000 – 2013 and 5,900km<sup>2</sup> in 2013 – 2022. Appendix 1 provides an overview of changes by category during each time-interval.

### **3.3. Land-cover change budget**

In the context of land-cover change accounting, a budget was created per land category to provide insights into the gains, losses and persistence for that category during both time-intervals. Each category's gains, losses and persistence are depicted in Fig. 4a-g. Otherland (Fig. 4b), artificial surface (Fig. 4c), cropland (Fig. 4e) and grassland (Fig. 4f) are net-gaining categories during both time intervals, whereas tree-covered area (Fig. 4g) was a net-losing category across both time-intervals. In contrast, wetland and waterbody were net-losing categories in 2000 – 2013 but net-gaining in 2013 – 2022.

### **3.4 Multi-level intensity of land-cover changes from 2000 – 2013 to 2013 – 2022**

The intensity of annual change during an interval, capturing the speed of land transformation, increased from 3.3% in 2000 – 2013 to 4.5% in 2013 – 2022. We further quantified the intensity at which land-cover change occurred at the category level and by AEZs (Fig. 5). Fig. 5a. depicts the observed intensity of annual gross gain for each category during both time-intervals. The annual change intensity among land-cover categories (Fig. 5a) increased from 2000 – 2013 to 2013 – 2022 for all categories. Thus, annual change intensities were higher in the second time-interval than in the first time-interval. Otherland had the highest intensity during 2000 – 2013 (6.1% yr<sup>-1</sup>) and 2013 – 2022 (8.7% yr<sup>-1</sup>). At the level of the AEZs, annual change intensity mainly increased from 2000 – 2013 to 2013 – 2022, similar to the increasing trends at the category level. Intensities

were higher during 2013 – 2022 in all AEZs except SS and SaS whose rates were higher in 2000 – 2013.

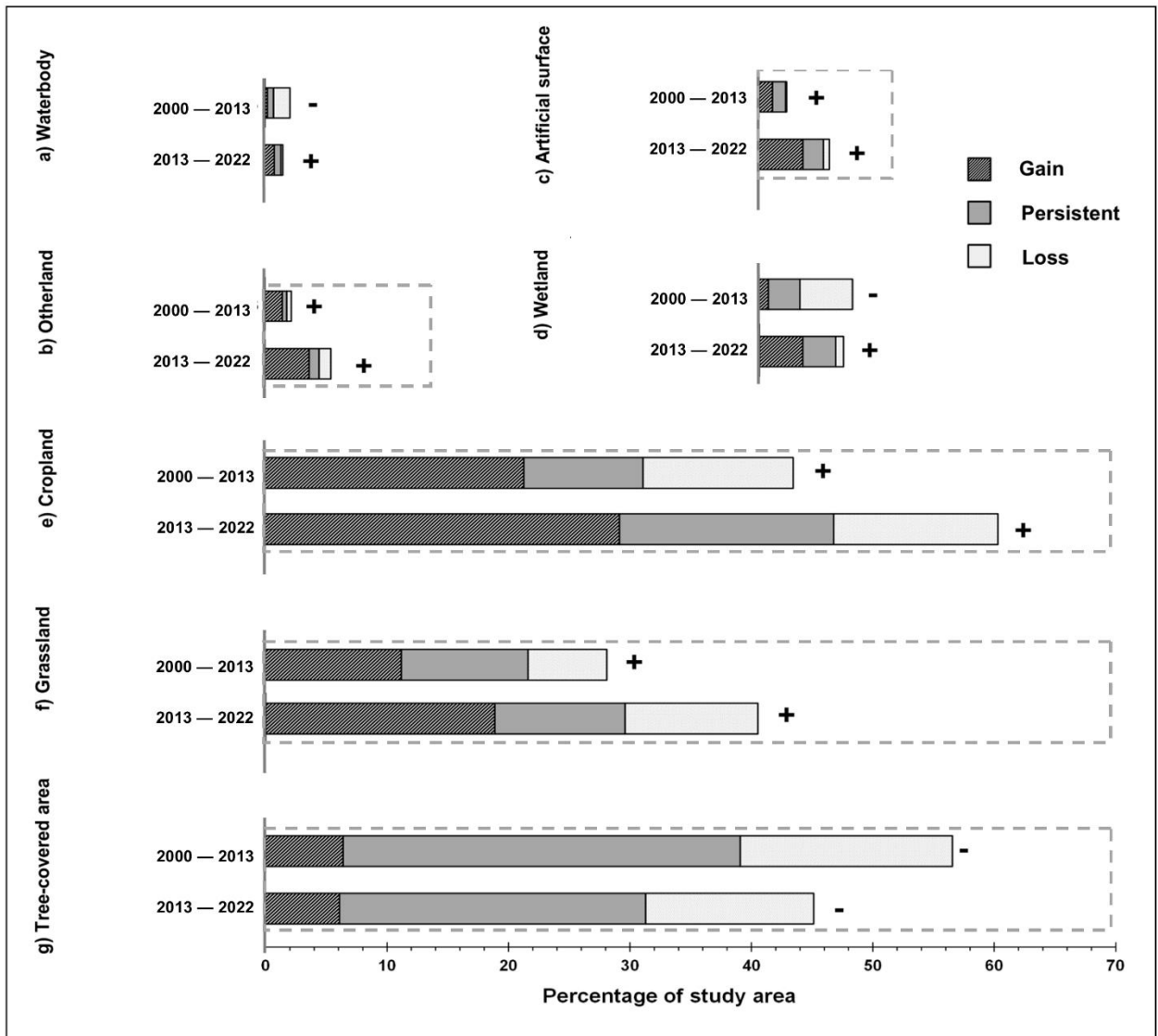


Figure 4. The change budget per land-cover category during both time-interval (2000 – 2013, 2013 – 2022). The budget depicts each category's gains, persistence and losses as a percent of the study area (+ means net gain, – means net loss).

The highest change intensity was found in the mangrove zone which increased from 7.3% yr<sup>-1</sup> in 2000 – 2013 to 10.5% yr<sup>-1</sup> in 2013 – 2022, whereas for RaF, intensity increased from 7.4% yr<sup>-1</sup> to 10.1% yr<sup>-1</sup> over the same periods.

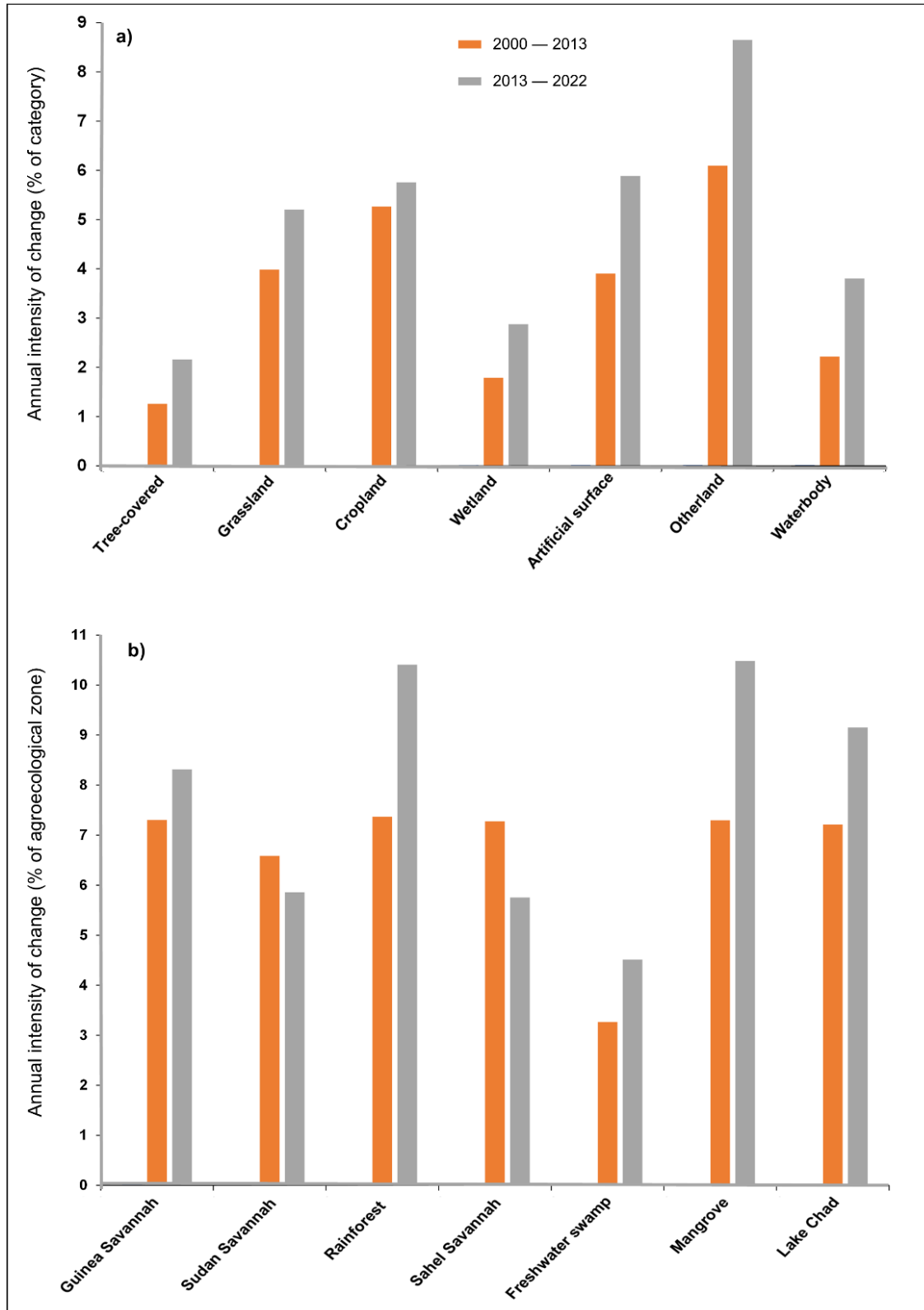


Figure 5. Annual observed intensity of change during two time-intervals, 2000 – 2013, 2013 – 2022, a) Annual gross gain of land-cover categories, b) Agroecological zones

### 3.5 Agroecological zone gradients of land-cover change

The proportion of land in areas of change and persisting land-cover in AEZs are depicted in Fig. 6. See Fig. S1 for change areas without persisting land-cover.

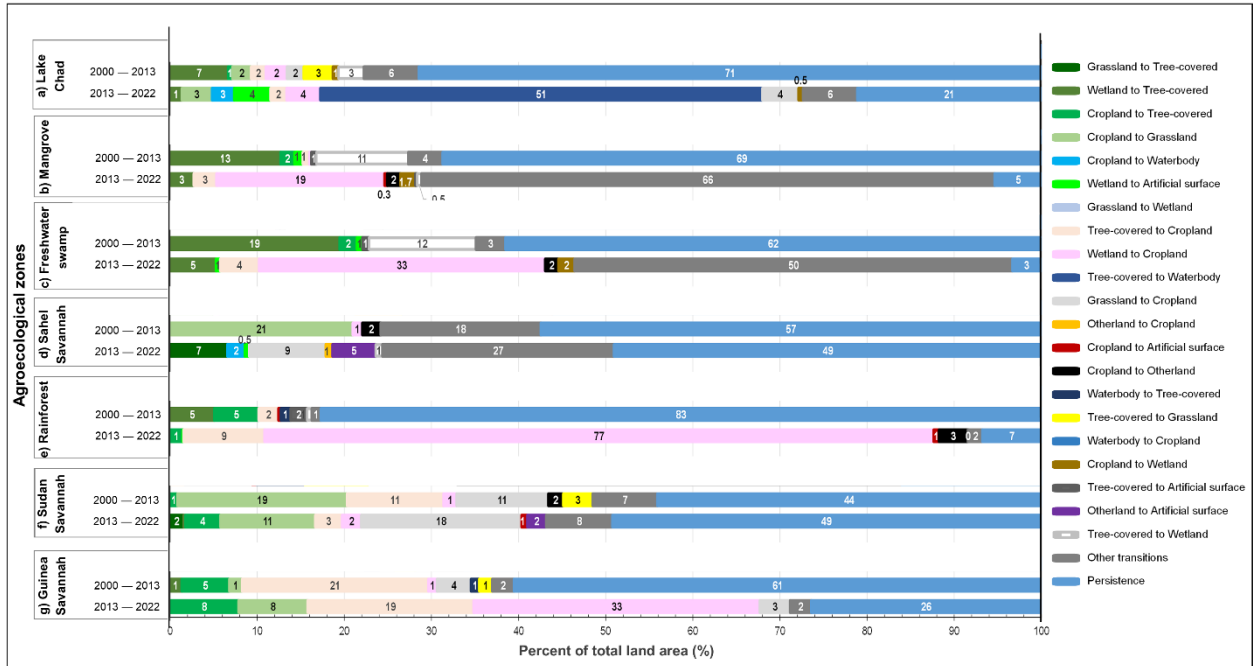


Figure 6. Persisting and major land-cover transitions by agroecological zones during 2000 – 2013 and 2013 – 2022.

Wetland conversion to cropland was higher during 2013 – 2022 in RaF (77%), FWS (33%), GS (33%), and mangrove (19%). Tree-cover loss to cropland was higher in 2000 – 2013 in GS (21%) and SS (11%), whereas tree-cover gains from cropland was higher in 2013 – 2022 in GS (8%). The conversion of croplands to grasslands was highest in the SaS (21%) and SS (19%) during 2000 – 2013. Wetland conversion to tree-cover was higher during 2000 – 2013 in FWS (19%) and mangrove (13%). Many persistent areas were lost over time. Persistent areas in the mangrove zone reduced from 69% in 2000 – 2013 to 5% in 2013 – 2022. In contrast, persistent areas in SS increased from 44% in 2000 – 2013 to 49% in 2013 – 2022.

### 3.4. Human appropriation of natural land-covers

We differentiated NLCs from HLU and aggregated these changes into three HANLC classes, 1) Cropland expansion, 2) Settlement and infrastructure development (SID), 3) Natural regeneration and afforestation (NRA).

### 3.4.1. Trajectories of natural and human-appropriated land-cover

Nine trajectories of HANLC were identified in each time-interval (Fig. 7). Fig. 7 depicts the three most prominent ones. NLC displacement by cropland decreased from 196,000km<sup>2</sup> (21.7%) in 2000 – 2013 to 167,000km<sup>2</sup> (18.4%) in 2013 – 2022, whereas NLC displacement by SID increased from approximately 7800 km<sup>2</sup> (0.9%) in 2000 – 2013 to 11,000km<sup>2</sup> (1.2%) in 2013 – 2022. Cropland displacement by SID increased from 200km<sup>2</sup> (0.03%) in 2000 – 2013 to 6000km<sup>2</sup> (0.7%) in 2013 – 2022. Settlement persistence increased from 10,000km<sup>2</sup> (1.1%) in 2000 – 2013 to 17,195km<sup>2</sup> (1.9%) in 2013 – 2022. NRA increased from 105,000km<sup>2</sup> (11.7%) over croplands and 400km<sup>2</sup> (0.04%) over settlements in 2000 – 2013 to 120,000km<sup>2</sup> (13.4%) over croplands and 2,000km<sup>2</sup> (0.1%) over settlements in 2013 – 2022. Despite the considerable amount of persisting NLC, it reduced from about 490,000km<sup>2</sup> (54.2 %) in 2000 – 2013 to 410,000km<sup>2</sup> (45.6%) in 2013 – 2022.

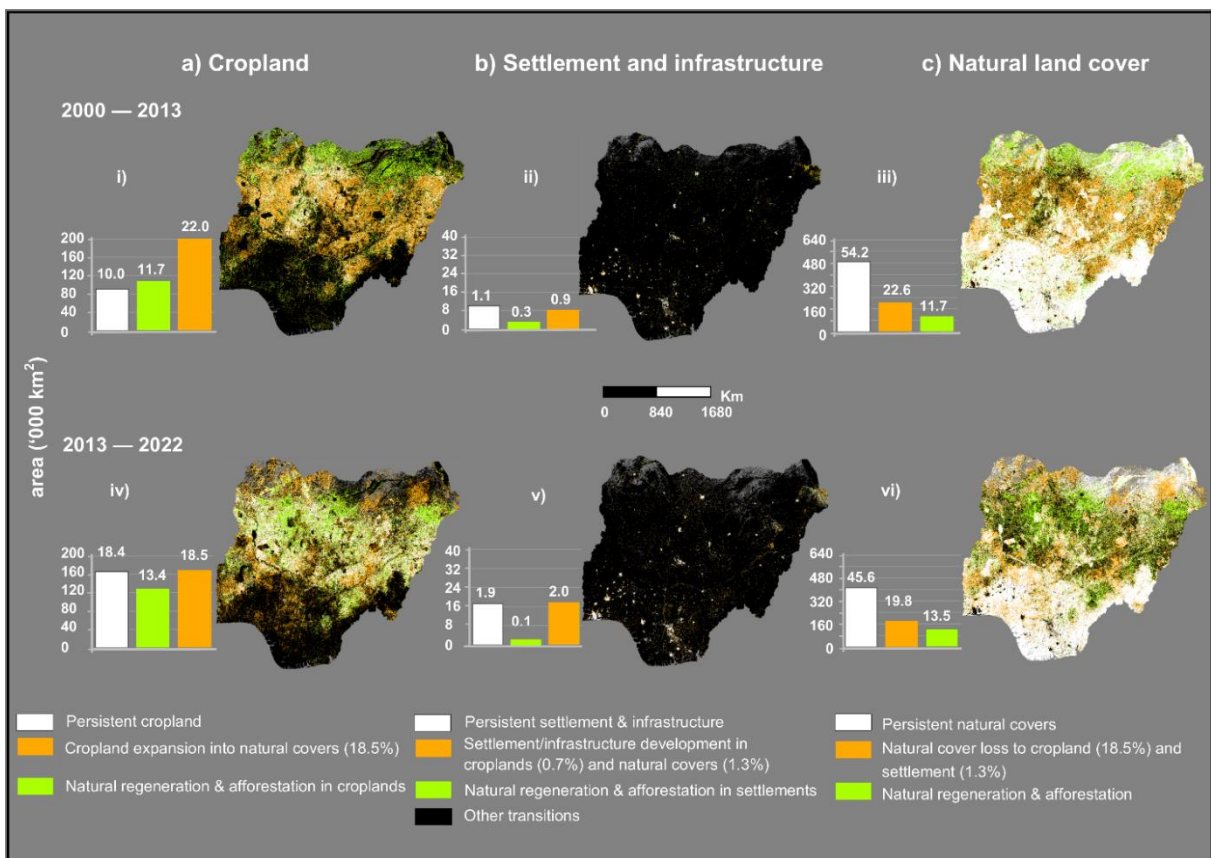


Figure 7. Major human-appropriated natural land-cover class ('000 km<sup>2</sup>) during 2000–2013 and 2013–2022 in areas of a) Cropland, b) Settlement and infrastructure c) Natural land-cover. Using 2013 – 2022 as an example, actual percentages were shown in the legend to highlight how the values of the land-cover transitions between the classes match. For example, 18.5% of cropland expansion into natural land-cover in 2013 – 2022 (Fig. a-iv) is a subset of the 19.8% lost by natural cover in Fig. c-vi.

### 3.4.2. Agroecological zone gradient of HANLC processes and drivers

We related observed HANLC change patterns to drivers and processes underlying these changes in each AEZ (Fig. 8). Fig. 8 depicts the extent of these broad HANLC changes across AEZs (less aggregated values of HANLC changes are provided as supporting information).

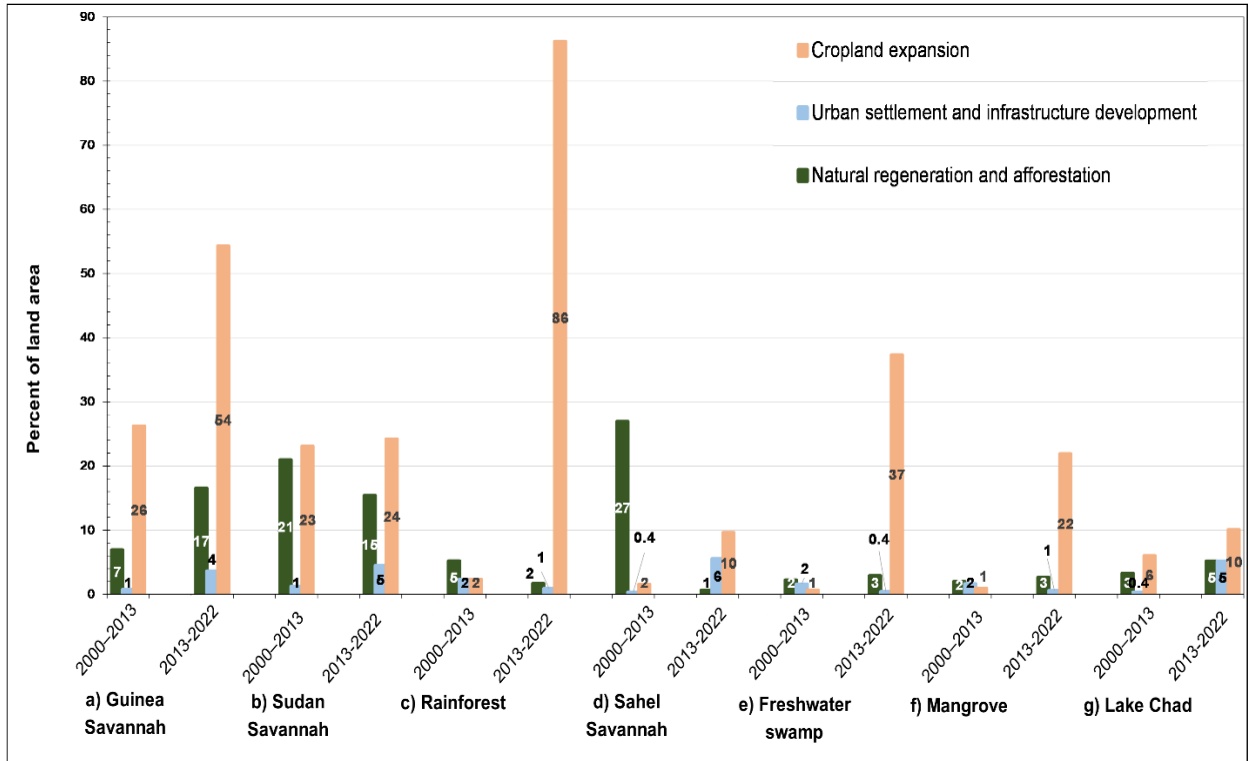


Figure 8. Extent of human-appropriated natural land-cover in agroecological zones

Details of the drivers and processes are provided in Table 5. Table 5 shows values for individual HANLC changes. The NRA process, for example, through tree-cover regeneration in croplands, drove changes to land-cover.

Table 5. HANLC changes expressed as percent of total land area in agroecological zones, where the upper number is 2000 – 2013 and the lower number is 2013 – 2022.

Drivers and Processes underlying HANLC changes		Agroecological zones (%)							
		Time Intervals	Guinea Savannah	Sudan Savannah	Rainforest	Sahel Savannah	Freshwater swamp	Mangrove	Lake Chad
*Natural regeneration and afforestation	Tree-cover expansion into cropland	2000 – 2013	5.48	0.84	5.09	0.01	1.99	1.60	0.49
		2013 – 2022	7.86	4.03	1.44	0.07	0.39	0.63	0.76
	Internal conversion of natural land	2000 – 2013	0.00	0.00	0.06	0.00	0.01	0.02	0.00
		2013 – 2022	0.01	0.06	0.01	0.14	0.02	0.03	0.04
	Expansion of grasslands into cropland	2000 – 2013	1.45	19.47	0.04	20.97	0.03	0.03	2.15
		2013 – 2022	7.93	10.89	0.02	0.38	0.01	0.04	3.47
Wetland expansion into cropland	2000 – 2013	0.01	0.07	0.02	0.05	0.21	0.34	0.64	
	2013 – 2022	0.66	0.29	0.19	0.01	1.84	1.72	0.27	
Settlement and infrastructure development	Settlement development over cropland	2000 – 2013	0.19	0.42	0.28	0.05	0.13	0.07	0.05
		2013 – 2022	0.83	0.67	0.62	0.03	0.28	0.31	0.15
	Settlement development over tree-cover	2000 – 2013	0.44	0.35	1.89	0.05	0.75	0.57	0.09
		2013 – 2022	0.22	0.06	0.13	0.00	0.05	0.16	0.04
	Settlement development over other covers	2000 – 2013	2.46	2.74	0.07	5.04	0.03	0.06	4.56
		2013 – 2022	13.61	1.64	5.72	0.00	2.07	1.99	1.65
Cropland expansion	Cropland expansion into tree-cover	2000 – 2013	21.38	11.09	2.27	0.10	0.48	0.77	1.69
		2013 – 2022	19.05	3.08	9.30	0.04	4.46	2.60	1.85
	Cropland expansion into grassland	2000 – 2013	3.91	10.53	0.01	0.38	0.01	0.00	1.92
		2013 – 2022	2.37	18.41	0.08	8.79	0.03	0.03	4.14
	Cropland expansion into wetland	2000 – 2013	0.96	1.50	0.07	1.10	0.20	0.20	2.42
		2013 – 2022	32.87	2.19	76.80	0.04	32.83	19.29	3.87
Land-cover degradation	NLC degradation (e.g., tree-cover loss to grassland and otherland)	2000 – 2013	0.00	0.59	0.00	5.92	0.00	0.00	0.02
		2013 – 2022	0.06	0.13	0.01	0.04	0.10	0.14	0.65
	Cropland degradation through conversion to otherland	2000 – 2013	0.00	0.00	0.00	0.00	0.00	0.00	0.00
		2013 – 2022	0.02	0.56	0.00	0.77	0.01	0.01	0.23

\* The computation of natural regeneration and afforestation are limited to only areas where natural cover expanded into human activity-related covers. NLC - Natural land-cover

The type of NRA differed between tree-cover or grassland expansion into croplands. The former was highest in the GS (5.5% in 2000 – 2013 and 7.9% in 2013 – 2022). In contrast, grassland expansion into cropland which was higher in 2000 – 2013 than in 2013 – 2022 was approximately 21% in SaS and 19.5% in SS. Despite the limited land area involved, SID expansion drove NLC decline, mainly over tree-cover in 1.9% of the total area of the RaF in 2000 – 2013, whereas SID encroached into other NLCs aside tree cover in GS (13.6%) and RaF (5.7%) in 2013 – 2022. In contrast, cropland expansion into NLC (e.g., tree-cover) was highest in GS during 2000 – 2013 (21.4%), whereas it was 19% in 2013 – 2022. In contrast, the loss of wetlands to croplands was

higher in 2013 – 2022 in these four AEZs and in this order, RaF (76.8%), GS and FWS (32.8%), and mangrove (19.3%). NLC degradation (e.g., tree-cover loss to otherlands signifying land degradation), was highest in SS (5.9%) in 2000 – 2013 than in any other AEZ. Although cropland degradation, leading to conversion into otherland, was minimal, values were higher in 2013 – 2022 in SaS (0.77%) and in SS (0.6%).

## **4. DISCUSSION**

### **4.1. Image classification and land-cover mapping**

Maintaining the same methods necessitated using only data from Landsat as it had the longest record. Consequently, this study did not use higher-resolution multispectral images such as Sentinel-2. There were seasonal variations in vegetation cover and perpetual cloud cover in AEZs such as mangrove, FWS and RAF. Hence, only multiyear composites were used for mapping land-cover instead of single or monthly composites. The low OA recorded in 2000 is probably related to the excessive cloud cover in the composite. Including the median values of each LSR band, NDVI, NDBI and MNDWI in the composites improved the classification results. Our findings, however, differed from most previous studies (e.g., Grigoras et al., 2019; Alademomi et al., 2022) in that the effect of NDBI on the image classification for Nigeria was negligible or sometimes reduced the accuracy.

Identifying artificial surfaces and wetlands was difficult, especially for rural settlements in highly forested regions in RaF. Wetlands were difficult to distinguish from cropland when cultivated. Other affected categories are croplands, which were mostly confused with tree-covered areas in RaF. In these tropical forest-agriculture mosaic landscapes, trees and tree-crops on the farms and the small farm sizes made differentiating croplands from tree-covered areas difficult.

### **4.2. The intensity and drivers of land transformation**

This study assessed and characterized persisting land-cover and change across Nigeria (2000 – 2022). It differentiated the 23-year study period into two time-intervals (i.e., 2000–2013, 2013–2022). Land-cover types such as cropland, grassland, otherland and artificial surfaces were net gaining categories as these expanded into other categories, whereas tree-covered area was a net losing category. Further, we examined the change intensity at the interval and category levels and by AEZ. Results from the interval level analysis revealed that the intensity of annual change increased from the first to the second time-interval. This implies that the speed at which land was

transformed accelerated during the last decade in Nigeria. The increasing intensity of annual change in all AEZs from 2000 – 2013 to 2013 – 2022 further confirms this trend except in SS and SaS where the intensity was higher in 2000 – 2013. Our analysis of the transitions involving cropland reveals that the higher intensity of change in the SS and SaS during 2000 – 2013 was mainly due to cropland expansion into grasslands and otherlands. Cropland expansion into grasslands and otherlands in these arid AEZs in 2000 – 2013 was made possible by irrigation schemes, e.g., Talata Mafara on Sokoto-Rima river basins (Adelodun and Choi, 2018). This trend of cultivating otherlands and grasslands was also found in Egypt, Algeria, Morocco (Molotoks et al., 2018; Bouaroudj et al., 2019).

Cropland occupied 37% of the land area in Nigeria as of 2022, mainly due to expansion into tree-cover and grasslands, especially in the GS, RaF, FWS and mangroves during 2013 – 2022. Forty-six (46%) and 18% of cropland areas in 2000-2013 were derived from tree-cover and grasslands and in 2013 – 2022, 30% and 20% of cropland areas were in displaced tree-cover and grasslands. Confirming cropland to be the main land-use in Nigeria, our estimate of cropland extent aligns closely with the CIA (2023) estimates of 37.3% for arable land as of 2018, whereas FAO (2020) estimate was 42% as of 2016. That majority of existing croplands persisted is confirmed by Onilude and Vaz (2020), which found greater cropland compactness. Agriculture is an essential economic sector in Nigeria, accounting for 24% of the GDP in 2020, with 70% of its over 200 million population dependent on it (Yakubu and Akanegbu, 2015).

As croplands expanded in Nigeria, so were they lost due to settlement expansion, tree-cover and grassland through land degradation processes. The loss of tree-cover and croplands to grassland signify land degradation as these agro- and forest ecosystems become grasslands (e.g., Adenle et al., 2022; Onilude and Vaz, 2020; Akinyemi and Ifejika Speranza, 2022). Urban built-up encroached agricultural rural landscapes, forests, and wetlands. Settlement expansion into wetlands occurred in all marine AEZs (e.g., FWS and mangrove), making urbanization a significant driver of wetland loss in Nigeria despite the limited land area. For example, the main feature of settlement expansion in the Lagos conurbation is wetland reclamation in the Lekki Peninsula and Eko Atlantic City (EAC 2012; Obiefuna et al. 2013).

In contrast, tree-covered area was a net losing category from 2000 to 2022 due to cropland and grassland expansion. In 2000 – 2013, 4.9% of tree-cover were displaced by grassland, whereas 4.2% of tree cover was lost to grassland in 2013 – 2022. The finding of a decreasing trend in tree-cover due to agriculture and grassland encroachment in 2000 – 2013 and 2013 - 2022 is corroborated by previous studies (e.g., Aruofor, 2001; Akinyemi, 2013; FAO, 2020). For example, tree-cover loss to cropland in GS and RaF can be partly attributed to policies favoring export-oriented cash cropping (e.g., the 1980 – 1990 trade liberalization policy) (Akinyemi, 2013).

Estimated as occupying 31% of Nigeria's land area in 2022, this study's estimate exceeded 2016 Hansen data-based forest estimate of 24% for Nigeria (FAO, 2020). This probably is because the tree-covered area class in the UNCCD scheme is broader, comprising forest, savanna, woodland, thicket and plantation.

Of all AEZs, the mangrove zone was the most disturbed as persisting areas reduced from 69% in 2000 – 2013 to 5% in 2013 – 2022. Mangrove forest loss is also driven by impacts of oil spills in the Niger Delta at the coast (Gundlach, 2018; Mzaga et al., 2021). Tree-cover loss in Nigeria is also driven by charcoal-induced deforestation (Omeje, 2021) due to charcoal production for domestic use and export (Van Wesenbeeck, 2016; Huitink, 2018; Salamatu et al., 2021). Huitink (2018) estimated that the 147 ktonnes of Nigerian charcoal imported into the European Union in 2016 would require about 120km<sup>2</sup> of forest cut with an assumption of tree harvest for producing charcoal without replanting. Results also show tree-cover gains in croplands in 2013 – 2022. This trend is confirmed by Azeez (2018) and Arowolo and Deng (2018). Azeez (2018) noted vegetation regrowth in croplands and settlements in areas where civil conflict forced people to abandon land.

### **4.3. Human-appropriated natural cover**

Differentiating between NLC and HLU, we estimated how much humans have appropriated NLC over time (HANLC). Drivers and processes underlying HANLC changes were related largely to artificialization due to settlement and infrastructure development, cropland expansion resulting in NLC decline, and natural regeneration and afforestation. HANLC changes led mostly to declining NLCs due to conversion forests, wetlands and grasslands to cropland and settlements. The main drivers of NLC loss were agriculture-induced deforestation due to the conversion of tree-cover and grassland to cropland; wetland converted into croplands, artificial surfaces, and grassland degradation, resulting in primarily barelands. These results, revealing heightening socioeconomic and environmental pressures in Nigeria, are corroborated by previous studies (e.g., Salamatu et al., 2018; Herrmann et al., 2020). Studies confirm forest loss due to cropland expansion in other parts of Africa (e.g., Turubanova et al., 2018; Akinyemi and Ifejika Speranza, 2022).

NLC gains were limited despite expanding into croplands and some settlements during both time-intervals. NLC increase in croplands was highest in the SaS and SS during 2000 – 2013. This trend of NLC increase in the semi-arid AEZs is likely the result of natural regeneration, reforestation and afforestation efforts. This is confirmed by the greening trends of increasing woody species in some Sahelian countries (Mbow et al., 2015; West et al., 2017). Thus, the regeneration of NLC in croplands contributed to driving land-cover changes in Nigeria. For example, NLC expansion into croplands was highest in GS.

## 5. POLICY IMPLICATIONS AND CONCLUSIONS

Recent advances in satellite image data capture, free access, and geospatial cloud computing (Xu et al. 2020) enabled this study to create land-cover maps of 2000, 2013 and 2022 over Nigeria. Using the same methodologies and classification schemes, we made these 30m Landsat-based time-series of systematically produced land-cover datasets. This study filled the gap of a current national scale evaluation of land transformation in Nigeria, which is still lacking. An overview of how land-cover changed, the spatial extent and annual intensity of land-cover change at multilevels during two time-intervals (i.e., 2000 – 2013, 2013 - 2022). Improved knowledge of the Nigerian context is to be gained from this long-term assessment of human-appropriated natural land-cover. These analyses may better reflect the prevailing economic and policy contexts in which land transformation occurred. For example, the annual change intensity increased from 2000 – 2013 to 2013 – 2022, implying accelerating speed of land transformation.

As part of Nigeria's commitment to follow a low-carbon development path and transition towards Land Degradation Neutrality, it targeted zero forest and wetland loss and a 20% forest cover increase by 2020 compared to 2015 estimates (Government of Nigeria, 2018). However, Nigeria lost more natural land-covers between 2000 and 2022, so more concerted scientific, policy and societal efforts are urgently required to reverse this declining trend. The Nigerian economy grew 7.4% annually between 2000 and 2013 before reducing to 1.9% during 2013 – 2022 due to dwindling oil revenue, financial crises and COVID-19 impacts.

That cropland expanded in both time-intervals is reflected in agriculture's contribution to GDP in Nigeria which rose from 21.4% (2000), 23.3% (2013), 22% (2020) to 23.7% in 2022 (World Bank and OECD, 2023). Cropland expansion can be partly attributed to the focus of the agricultural and land policies implemented. For example, the 2012 Agricultural Transformation Agenda and Agricultural Promotion Policy (2015 – 2020) aimed at harnessing more arable lands for food production. Nigeria underwent a process of cropland extensification with an overall net decrease in yield per land area cultivated, like the situation in ~40% of African countries (Akinyemi and Ifejika Speranza, 2022). Ensuring that cropland intensification is sustainable is essential to harness the potential of existing croplands in Nigeria. Food must be produced environmentally-friendly without necessarily expanding croplands while preventing croplands from degrading (Adenle et al., 2017; Govers et al., 2017).

Much loss of croplands is related to natural regeneration, settlement expansion and land degradation. Major implications of agricultural land loss are that more remote and marginal lands tend to be farmed, resulting in more clearing of tree-cover and loss of grasslands which is not good for biodiversity that are acclimatized to grassland ecosystems (Akinyemi and Ifejika Speranza, 2022). Grassland conversion to cropland implies lower productivity as grasslands are mainly in

areas with lesser rainfall and lower soil fertility. To maintain or increase yields, an increasing need for external inputs (e.g., water and fertilizer) is likely. Since many African farmers are smallholders and resource-poor, accessing such inputs is a challenge hence the prospects for maintaining or improving food production based only on smallholders' capacities are low. Strong institutions are needed if broad-scale support that limits the environmental burdens of inputs is to be provided to farmers (Schouten et al., 2018) such as developing sustainable low-input agriculture (Poortinga et al., 2019).

The increasing urbanization trend in Nigeria during both time-intervals is confirmed by previous findings (e.g., Tappan et al., 2016; Arowolo and Deng, 2018; Onilude and Vaz, 2020). Settlement expansion in the southern part of Nigeria forms a part of the West African urbanization hotspots, extending along the coast from Monrovia (Liberia), Abidjan (Côte d'Ivoire), Accra (Ghana), Lagos, Ibadan, Benin-City, Onitsha (Nigeria) to Douala (Cameroon), a stretch of 3045 kilometers (Akinyemi and Ifejika Speranza, 2022).

This study did not cover how HANLC changes affect ecological sustainability over time and space over Nigeria. Despite this limitation, insights revealing the dominance of land-cover transitions to and from cropland, especially agriculture-induced tree-cover loss, provide a basis for future research. It is imperative to consider the effects of markets and trade in driving agricultural land change, especially impacts of telecoupled demand (i.e., distal) for land-based produce (e.g., cocoa and cassava). For example, the environmental impacts of tropical forest loss due to export-oriented agriculture illustrate the shift of the social-ecological burdens to the tropics (De Sy et al., 2015; Twongyirwe et al., 2018). This situation contrasts with ongoing forest management, afforestation, and agricultural abandonment in most of the global North (Yue et al., 2020; Winkler et al., 2021).

The contributions of this study are threefold. First is the creation of the most current land-cover products for Nigeria. With the use of the UNCCD classification scheme, results from this study are relevant for use in other domains requiring land-cover and land-cover change data over Nigeria. This reasonably accurate and timely information on the spatial distribution of seven land-cover types can be used to quantify the land-cover changes and their impacts when gauging Nigeria's commitments such as the Nationally Determined Contributions and National Action Programmes relating to the various Rio Conventions. Second is applying a multi-level assessment of the intensity of change patterns and the comparative assessment of these patterns between categories and agroecological zones across two time-intervals. Third, is the examination of the extent of human appropriated natural land-cover. Further research and investigations on scenarios of future land-cover dynamics relating to the processes identified are needed.

## Appendix 1: Change matrix in km2 (2000 – 2022)

	Category	Tree-covered	Grassland	Cropland	Wetland	Artificial surface	Otherland	Waterbody	Total
<b>Land area under each transition during the second time-interval (2000 – 2013)</b>									
<i>Latter time 2013</i>									
<i>Initial time</i> 2000	Tree-covered	297716.3	17375.7	130158.4	5724.8	5070.0	181.7	406.2	456633.1
	Grassland	1948.2	95011.0	49900.9	154.4	1209.9	5634.8	104.2	153963.4
	Cropland	32046.6	71591.9	89408.6	428.9	2461.9	5922.5	115.2	201975.7
	Wetland	18058.8	9123.4	9382.3	23853.6	985.5	1088.9	1244.0	63736.4
	Artificial surface	261.0	103.3	245.4	9.3	9965.9	3.6	0.8	10589.3
	Otherland	67.18	3191.8	53.1	6.2	13.1	3431.9	5.4	6768.5
	Waterbody	5879.2	630.9	4209.8	902.1	524.3	289.1	4628.4	17063.6
	2013 total	355977.2	197028.0	283358.4	31079.3	20230.6	16552.4	6504.1	910730
<b>Land area under each transition during the second time-interval (2013 – 2022)</b>									
<i>Latter time 2022</i>									
<i>Initial time</i> 2013	Tree-covered	229657.8	11919.3	100121.0	5318.1	6725.7	1288.8	657.7	355688.4
	Grassland	4171.9	97646.7	67418.1	2031.6	3916.8	21867.6	92.2	197144.9
	Cropland	46956.6	66486.9	160508.5	823.5	6201.5	2425.3	332.0	283734.3
	Wetland	2862.2	397.4	1256.3	24878.6	273.6	63.1	1224.8	30955.9
	Artificial surface	965.5	625.8	1614.2	106.1	15738.5	1004.0	198.3	20252.5
	Otherland	63.3	6324.0	1923.7	235.0	261.8	7613.5	69.7	16490.9
	Waterbody	363.9	273.6	265.9	178.7	340.8	89.1	4951.2	6463.2
	2022 total	285041.0	183673.7	333107.6	33571.6	33458.7	34351.4	7526.1	910730

## ACKNOWLEDGMENT

This research was conducted within the Land-use Change and the Resilience of Food Production Systems (LucFRes) project. This project has received funding from the European Union's Horizon 2020 research and innovation programme under the Marie Skłodowska-Curie grant agreement No 101025259. We are grateful for free access to all Landsat images, auxiliary datasets used, and open cloud geospatial processing tools in Google Earth Engine. This study contributes to the Global Land Programme (<https://glp.earth>) and the Programme on Ecosystem Change and Society (<https://www.pecs-science.org>). All content and information contained in this article reflect only the authors' views and not that of the EU, the European Union's Horizon 2020 or any other body.

**Disclosure statement:** No potential conflict of interest was reported by the authors.

**Data availability:** Sources of all datasets used are specified in the manuscript and are provided as supplementary information (later this will be uploaded upon acceptance in Zenodo <https://doi.org/10.5281/zenodo.8205099>).

## ORCID:

Felicia O. Akinyemi <https://orcid.org/0000-0001-6248-7430>

C. Ifejika Speranza <https://orcid.org/0000-0003-1927-7635>

## REFERENCES

Adelodun, B., Choi, K-S. 2018. A review of the evaluation of irrigation practice in Nigeria: Past, present and future prospects. *African Journal of Agricultural Research*, 3EAF05558713 <http://dx.doi.org/10.5897/AJAR2018.13403>

Adenle, A.A., Azadi, H., Manning, L., 2017. The era of sustainable agricultural development in Africa: understanding the benefits and constraints. *Food Rev. Int.* doi:10.1080/87559129.2017.1300913.

Adenle, A.A., Boillat, S., Ifejika Speranza, C. 2022. Key dimensions of land users' perceptions of land degradation and sustainable land management in Niger State, Nigeria. *Environmental Challenges* 8, 100544, <https://doi.org/10.1016/j.envc.2022.100544>.

Akinyemi, F.O. 2013. An assessment of land use change in the cocoa belt of south west Nigeria. *International Journal of Remote Sensing* 34(8):2858-2875. <https://doi.org/10.1080/01431161.2012.753167>

Akinyemi and Ifejika Speranza, 2022. Agricultural landscape change impact on the quality of land: An African continent-wide assessment in gained and displaced agricultural lands. *International Journal of Applied Earth Observation and Geoinformation* 106:102644. <https://doi.org/10.1016/j.jag.2021.102644>.

Alademomi, A.S., Okolie, C.J., Daramola, O.E., Akinnusi, S.A., Adediran, E., Olanrewaju, H.O., Alabi, A.O., Salami, T.J., Odumosu, J. 2022. The interrelationship between LST, NDVI, NDBI, and land cover change in a section of Lagos metropolis, Nigeria. *Applied Geomatics* 14, 299–314. <https://doi.org/10.1007/s12518-022-00434-2>

Aldwaik, S., Pontius, R.G. Jr, 2012. Intensity analysis to unify measurements of size and stationarity of land changes by interval, category, and transition. *Landscape and Urban Planning* 106:103–114. <https://doi.org/10.1080/13658816.2013.787618>

Aldwaik, S., Pontius, R.G. Jr, 2013. Map errors that could account for deviations from a uniform intensity of land change. *International Journal of Geographical Information Science*, 27(9), 1717–1739.

Akinyemi, F.O., Mashame, G. 2018. Analysis of land change in the dryland agricultural landscapes of eastern Botswana. *Land Use Policy* 76:798-811. <https://doi.org/10.1016/j.landusepol.2018.03.010>.

Alexander, P., Brown, C., Arneth, A., Finnigan, J. 2016. Human appropriation of land for food: the role of diet. *Global Environmental Change* 41, 88 - 98. <https://doi.org/10.1016/j.gloenvcha.2016.09.005>

Arowolo, A.O., Deng, X. 2018. Land use / land cover change and statistical modelling of cultivated land change drivers in Nigeria. *Regional Environmental Change* 18:247–259. <https://doi.org/10.1007/s10113-017-1186-5>

Azeez, O. 2018. *Once upon a game reserve: Sambisa and the tragedy of a forested landscape*. Arcadia Collection: National Parks in time and space, Spring 2018, no. 2. <http://www.environmentandsociety.org/arcadia/once-upon-game-reserve-sambisa-and-tragedy-forested-landscape> [access: 2023 Aug. 01].

Barnieh, B.A., Jia, L., Menenti, M., Jiang, M., Zhou, J., Lv, Y., Zeng, Y., Bennour, A. 2022. Quantifying spatial reallocation of land use/land cover categories in West Africa. *Ecological Indicators* 135, 108556. <https://doi.org/10.1016/j.ecolind.2022.108556>.

Breiman, L. 2001. Random forests. *Machine Learning* 45:5-32. <https://doi.org/10.1023/A:1010933404324>

Canty, M.J. 2019. *Image Analysis, Classification and Change Detection in Remote Sensing: With Algorithms for Python* (4th ed.), CRC Press, Taylor & Francis Group: Boca Raton, FL, USA.

CIA - Central Intelligence Agency 2023. Nigeria: The World Factbook. <https://www.cia.gov/the-world-factbook/countries/nigeria/> [access: 2023 Sept. 02].

Cotillon, S.E., and Mathis, M.L. 2017. *Mapping land cover through time with the Rapid Land Cover Mapper—Documentation and user manual*. US Geological Survey Open-File Report 1012, 23 p. <https://doi.org/10.3133/ofr20171012>

Cushing, W.M, Tappan, G.G., Herrmann, S., Cotillon, S.E. 2016. West Africa Land Use Land Cover Time Series. Earth Resources Observation and Science (EROS) Center. <https://doi.org/10.5066/F73N21JF>

De Sy, V., Herold, M., Achard, F., Beuchle, R., Clevers, J.G.P.W., Lindquist, E., & Verchot, L. 2015. Land use patterns and related carbon losses following deforestation in South America. *Environ. Res. Lett.* 10:124004. doi: 10.1088/1748-9326/10/12/124004.

Department of Drought and Desertification Amelioration, 2018. Nigeria final report of the Land Degradation Neutrality Target Setting Programme. [https://knowledge.unccd.int/sites/default/files/ldn\\_targets/Nigeria%20LDN%20TSP%20Country%20Report.pdf](https://knowledge.unccd.int/sites/default/files/ldn_targets/Nigeria%20LDN%20TSP%20Country%20Report.pdf) [access: 2023 Oct. 23].

EAC, 2012. *Environmental and social impact assessment of the Eko Atlantic shoreline protection and reclamation project a Summary*. Royal Haskoning Enhancing Society <https://www.ekoatlantic.com/wp-content/uploads/2012/12/EkoAtlantic-EIA-Summary.pdf> [access: 2023 Aug. 01].

FAO 2020. Land use/land cover and forest cover mapping in Nigeria. Abuja. <https://doi.org/10.4060/cb1327en> [access: 2023 Oct. 23].

Findell, K.L., Berg, A., Gentine, P., Krasting, J., Lintner, B.R., Malyshev, S., Santanello Jr., J.A., Shevliakova, E. 2017. The impact of anthropogenic land use and land cover change on regional climate extremes. *Nat Commun* 8, 989. <https://doi.org/10.1038/s41467-017-01038-w>

Government of Nigeria 2018. Report from Nigeria. UNCCD performance review and assessment of implementation system 7th reporting process. [https://prais.unccd.int/sites/default/files/pdf\\_reports/unccd\\_Nigeria\\_2018\\_1.pdf](https://prais.unccd.int/sites/default/files/pdf_reports/unccd_Nigeria_2018_1.pdf) [access: 2023 Aug. 01].

Govers, G., Merckx, R., van Wesemael, B., van Oost, K., 2017. Soil conservation in the 21st Century: why we need smart agricultural intensification. *Soil* 3, 45–59. <http://dx.doi.org/10.5194/soil-3-45-2017>.

Grigoras G., Uritescu, B. 2019. Land use/land cover changes dynamics and their effects on surface urban heat island in Bucharest, Romania. *Int J Appl Earth Obs Geoinf* 80, 115–126. <https://doi.org/10.1016/j.jag.2019.03.009>

Gundlach, E.R. 2018. Oil-related mangrove loss east of Bonny River, Nigeria. In: Makowski, C., Finkl, C. (eds) *Threats to mangrove forests*. Coastal Research Library, vol 25. Springer, Cham. [https://doi.org/10.1007/978-3-319-73016-5\\_13](https://doi.org/10.1007/978-3-319-73016-5_13)

Herrmann, S.M., Brandt, M., Rasmussen, K., Fensholt, R., 2020. Accelerating land cover change in West Africa over four decades as population pressure increased. *Communications Earth and Environment* 1:1–10. <https://doi.org/10.1038/s43247-020-00053-y>

Huitink, CL 2018. Burning Nigerian forests on European barbecues: A carbon footprint and cost comparison between imported Nigerian charcoal and sustainably produced charcoal in the European Union. Master thesis, Faculty of Geosciences, Utrecht University. <https://studenttheses.uu.nl/handle/20.500.12932/29543> [access: 2023 Oct. 23].

Ifejika Speranza, C., Akinyemi, F.O., Baratoux, D., Benveniste, J., Ceperley, N., Driouech, F., Helmschrot, J. 2023. Enhancing the uptake of earth observation products and services in Africa through a multi-level transdisciplinary approach. *Survey in Geophysics* 44:7–41 <https://doi.org/10.1007/s10712-022-09724-1>

Iloeje, N.P. 2001. A new geography of Nigeria (new revised edition). Longman Nig. Ltd:Lagos, Nigeria, p.200.

Jimoh, S.O., Muraina, T.O., Bello, S.K., NourEldeen, N. 2020. Emerging issues in grassland ecology research: Perspectives for advancing grassland studies in Nigeria. *Acta Oecologica* 106,103548. doi:10.1016/j.actao.2020.103548

Löw, F., Conrad, C., Michel, U. 2015. Decision fusion and non-parametric classifiers for land use mapping using multi-temporal RapidEye data. *ISPRS Journal of Photogrammetry and Remote Sensing* 108, 191–204. doi:10.1016/j.isprsjprs.2015.07.001

Mack, B., Leinenkugel, P., Kuenzer, C., Dech, S. 2017. A semi-automated approach for the generation of a new land use and land cover product for Germany based on Landsat time-series and Lucas in-situ data. *Remote Sensing Letters* 8(3), 244–53.

Main-Knorn M., B. Pflug, J. Louis, V. Debaecker, U. Müller-Wilm, F. Gascon 2017. Sen2Cor for Sentinel-2. *Proc. SPIE 10427, Image and Signal Processing for Remote Sensing XXIII*, 1042704.

Mbow, C., Brandt, M.S., Ouedraogo, I., de Leeuw, J., Marshall, M. 2015. What four decades of earth observation tell us about land degradation in the Sahel? *Remote Sensing*, 7(4), 4048–4067. doi:10.3390/rs70404048

McRoberts, R.E., Stehman, S.V., Liknes, G.C., Næsset, E., Sannier, C., Walters, B.F. 2018. The effects of imperfect reference data on remote sensing assisted estimators of land cover class proportions. *ISPRS Journal of Photogrammetry and Remote Sensing* 142: 292–300. <https://doi.org/10.1016/j.isprsjprs.2018.06.002>

Mzaga, T.M., Tse, A.C., Nwankwoala, H.O., Udom, G.J. 2021. Evaluating the impact of artisanal crude oil refining on soil properties at a mangrove wetland , eastern Bonny River, Rivers State. *International Journal of Research in Engineering and Science* 9(12):6-14.

Obiefuna, J.N., Nwilo, P., Atagbaza, A.O., Okolie, C.J. 2013. Land cover dynamics associated with the spatial changes in the wetlands of Lagos/Lekki Lagoon system of Lagos, Nigeria. *Journal of Coastal Research* 29(3):671-679. doi:10.2112/JCOASTRES-D-12-00038.1

Omeje, C. 2021. Do you know where your grilling charcoal comes from? Nigeria's forests are being decimated to make charcoal for cookouts in Europe and the United States. <https://newrepublic.com/article/161947/nigeria-where-does-grill-charcoal-come-from>

Onilude, O.O., Vaz, E. 2020. Data analysis of land use change and urban and rural impacts in Lagos State, Nigeria. *Data* 5(3):72. doi:10.3390/data5030072

Pelletier, C., Valero, S.; Inglada, J.; Champion, N.; Dedieu, G. 2016. Assessing the robustness of Random Forests to map land cover with high resolution satellite image time series over large areas. *Remote Sensing of Environment* 187, 156–168.

Pesaresi, M., Politis, P. 2023. GHS-BUILT-C R2023A - GHS Settlement Characteristics, derived from Sentinel2 composite (2018) and other GHS R2023A data. European Commission, Joint Research Centre (JRC). doi: 10.2905/3C60DDF6-0586-4190-854B-F6AA0EDC2A30

Pons, X., Pesquer, L., Cristobal, J., Gonzalez-Guerrero, O. 2014. Automatic and improved radiometric correction of Landsat imagery using reference values from MODIS surface reflectance images. *International Journal of Applied Earth Observation and Geoinformation*, 33, 243e254. <http://dx.doi.org/10.1016/j.jag.2014.06.002>

Poortinga A, Nguyen Q, Tenneson K, Troy A, Saah D, Bhandari B, Ellenburg WL, Aekakkarunroj A, Ha L, Pham H, Nguyen G, Chishtie F 2019. Assessing the Food Security Situation in Vietnam: A Landscape Approach. *Front Environ Sci* <https://doi.org/10.3389/fenvs.2019.00186>

Salamatu, E.A., Ayuba, H.K., Marcus, D.N., Ogah, A.T. 2021. Analysis of tree species preference and reasons among commercial charcoal producers in Nasarawa state, Nigeria. *European Journal of Environment and Earth Sciences* 2(2):24-29. <https://doi.org/10.24018/ejgeo.2021.2.2.124>

Schonlau, M., Zou, R.Y. 2020. The random forest algorithm for statistical learning. In: *The Stata Journal: Promoting communications on statistics and Stata* 20(1):3–29.

Schouten G, Vink M, Vellema S 2018. Institutional diagnostics for African food security: Approaches, methods and implications. *Wageningen Journal of Life Sciences* 84:1-5 <https://doi.org/10.1016/j.njas.2017.11.002>

Sims, N.C., Newnham, G.J., England, J.R., Guerschman, J., Cox, S.J.D., Roxburgh, S.H., Viscarra Rossel, R.A., Fritz, S., Wheeler, I. 2021. Good Practice Guidance. SDG Indicator 15.3.1, proportion of land that is degraded over total land area. v2.0. United Nations Convention to Combat Desertification, Bonn, Germany.

Tappan, G.G., Cushing, W.M., Cotillon, S.E., Mathis, M.L., Hutchinson, J.A., Dalsted, K.J. 2016. West Africa land use land cover time series: US Geological Survey data release.

Turubanova, S., Potapov, P.V., Tyukavina, A., Hansen, M.C. 2018. Ongoing primary forest loss in Brazil, Democratic Republic of the Congo, and Indonesia. *Environmental Research Letters* 13(7):074028.

Twongyirwe, R., Bithell, M., Richards, K.S. 2018. Revisiting the drivers of deforestation in the tropics: Insights from local and key informant perceptions in western Uganda. *Journal of Rural Studies* 63:105–119.

UNCCD 2019. Land Degradation Neutrality Transformative Projects and Programmes: Operational Guidance for Country Support. Global Mechanism of the UNCCD, Bonn, Germany. [https://catalogue.unccd.int/1224\\_UNCCD\\_LDN\\_TPP\\_technical\\_guide\\_GM.pdf](https://catalogue.unccd.int/1224_UNCCD_LDN_TPP_technical_guide_GM.pdf) [access: 2023 February 04].

UNFPA 2023. Nigerian population. <https://www.unfpa.org/data/world-population/NG> [access: 2023 October 23].

Van Wesenbeeck, S., Wang, L., Ronsse, F., Prins, W., Skreiberg, Ø., Antal Jr, M.J. 2016. Charcoal “Mines” in the Norwegian Woods. *Energy and Fuels* 30(10), 7959–7970. <https://doi.org/10.1021/acs.energyfuels.6b00919>

Wang, L., Wei, F., Svenning, J-C. 2023. Accelerated cropland expansion into high integrity forests and protected area. *iScience* 26(4), 106450. <https://doi.org/10.1016/j.isci.2023.106450>

West, C.T., Moody, A.J., Nébié, E.K., Sanon, O. 2017. Ground-truthing Sahelian Greening: Ethnographic and Spatial Evidence from Burkina Faso. *Hum Ecol Interdiscip J* 45(1):89–101. doi:10.1007/s10745-016-9888-8

Winkler, K., Fuchs, R., Rounsevell, M., & Herold, M. 2021. Global land use changes are four times greater than previously estimated. *Nat Commun* 12:1–10. <https://doi.org/10.1038/s41467-021-22702-2>

World Bank and OECD National Accounts data 2023. Agriculture % of GDP in Nigeria. <https://data.worldbank.org/indicator/NV.AGR.TOTL.ZS?view=chart&locations=NG> [access: 2023 Aug. 01].

Xu, C., Du, X., Yan, Z., Fan, X. 2020. ScienceEarth: A big data platform for remote sensing data processing. *Remote Sensing* 12, 607. <https://doi.org/10.3390/rs12040607>

Yakubu, M., Akanegbu, B. 2015. Neglecting agriculture and its consequences to the Nigerian economy: An analytical synthesis. *European Journal of Research in Social Sciences* 3, 18–27.

Young, N.E., Anderson, R.S., Chignell, S.M., Vorster, A.G., Lawrence, R., & Evangelista, P.H. 2017. A survival guide to Landsat preprocessing. *Ecology* 98(4):920e932.

Yue, C., Ciais, P., Houghton, R.A., Nassikas, A.A. 2020. Contribution of land use to the interannual variability of the land carbon cycle. *Nature Communications* 11:3170. <https://doi.org/10.1038/s41467-020-16953-8>

## Supplementary Information

### Land-cover transition matrix as percentage (2000 – 2022)

UNCCD classification scheme		1	2	3	4	5	6	7
		Tree-covered area	Grassland	Cropland	Wetland	Artificial surface	Otherland	Waterbody
<b>Percentage of land area under each transition during the second time interval (2000 – 2013)</b>								
<i>Latter time 2013</i>								
<i>Initial time 2000</i>	<b>Tree-covered area</b>	83.6	8.8	45.9	18.4	25.1	1.1	6.2
	<b>Grassland</b>	0.6	48.2	17.6	0.5	6	34	1.6
	<b>Cropland</b>	9	36.3	31.6	1.4	12.2	35.8	1.8
	<b>Wetland</b>	5.1	4.6	3.3	76.8	4.9	6.6	19.1
	<b>Artificial surface</b>	0.1	0.1	0.1	0	49.3	0	0
	<b>Otherland</b>	0	1.6	0	0	0.1	20.7	0.1
	<b>Waterbody</b>	1.7	0.3	1.5	2.9	2.6	1.8	71.2
<b>Percentage of land area under each transition during the third time interval (2013 – 2022)</b>								
<i>Latter time 2022</i>								
<i>Initial time 2013</i>	<b>Tree-covered area</b>	81.2	6.5	28.7	12	18.9	3.7	7.9
	<b>Grassland</b>	1.3	53.7	20.7	6.1	11	63	1
	<b>Cropland</b>	16.6	35.9	49.4	2.4	17.6	6.6	4
	<b>Wetland</b>	0.6	0.2	0.3	78.2	0.7	0.2	16.1
	<b>Artificial surface</b>	0.2	0.2	0.3	0.2	50.1	2.9	2.6
	<b>Otherland</b>	0.02	3.4	0.5	0.7	0.8	23.3	0.9
	<b>Waterbody</b>	0.1	0.1	0.08	0.3	1	0.26	67.4

**Error matrix and accuracy of land cover maps (2000 – 2022)**

<b>2000</b>	<b>Tree-covered areas</b>	<b>Grassland</b>	<b>Cropland</b>	<b>Wetland</b>	<b>Artificial Surfaces</b>	<b>Other land</b>	<b>Water body</b>	<b>Total</b>	<b>User accuracy (%)</b>
Tree-covered areas	80	13	33	0	0	0	1	127	0.63
Grassland	1	57	22	0	0	0	1	81	0.7
Cropland	10	20	52	0	0	0	0	82	0.63
Wetland	0	2	0	79	0	0	10	91	0.87
Artificial Surfaces	2	0	2	0	14	0	0	18	0.78
Otherland	0	0	0	0	0	14	1	15	0.93
Waterbody	1	0	0	0	0	0	85	86	0.99
Total	94	92	109	79	14	14	98	500	
P_Accuracy	0.85	0.62	0.48	1	1	1	0.87		0.76
<b>2013</b>									
Tree-covered areas	71	1	2	0	0	0	0	74	0.96
Grassland	1	28	1	0	0	7	0	37	0.76
Cropland	8	1	23	0	0	0	0	32	0.72
Wetland	0	0	0	26	0	0	2	28	0.93
Artificial Surfaces	0	0	2	0	10	0	0	12	0.83
Otherland	0	1	0	0	0	70	1	72	0.97
Waterbody	0	0	0	1	0	0	122	123	0.99
Total	80	31	28	27	10	77	125	378	
Producer accuracy	0.89	0.9	0.82	0.96	1	0.91	0.98		<b>0.93</b>
<b>2022</b>									
Tree-covered areas	13	4	5	0	0	0	0	22	0.59
Grassland	2	17	0	0	0	0	0	19	0.89
Cropland	0	12	50	0	0	2	0	64	0.78
Wetland	0	0	0	34	0	0	0	34	1
Artificial Surfaces	0	0	8	0	15	2	10	35	0.43
Otherland	0	3	2	0	0	11	0	16	0.69
Waterbody	0	0	0	0	0	0	115	115	1
Total	15	36	65	34	15	15	125	305	
Producer accuracy	0.87	0.47	0.77	1	1	0.73	0.92		<b>0.84</b>

Summary of human-appropriated natural land cover (HANLC) changes expressed as percent of total land area in agroecological zones. where the upper number is 2000 – 2013 and the lower number is 2013 – 2022.

**Agroecological zones (%)**

<b>Drivers and Processes underlying HANLC changes</b>	<b>Time Intervals</b>	<b>Guinea Savannah</b>	<b>Sudan Savannah</b>	<b>Rainforest</b>	<b>Sahel Savannah</b>	<b>Freshwater swamp</b>	<b>Mangrove</b>	<b>Lake Chad</b>
<b>*Natural regeneration and afforestation</b> (expansion of natural cover in croplands)	2000 – 2013	6.94	20.97	5.22	26.95	2.25	2.01	3.3
	2013 – 2022	16.56	15.41	1.7	0.65	2.92	2.66	5.2
<b>Settlement and infrastructure development</b> (e.g.. settlement expansion into natural cover and croplands)	2000 – 2013	0.78	1.24	2.37	0.37	1.6	1.65	0.37
	2013 – 2022	3.65	4.5	0.89	5.56	0.41	0.6	5.2
<b>Cropland expansion</b> (e.g.. loss of natural cover to croplands)	2000 – 2013	26.25	23.11	2.35	1.58	0.69	0.97	6.04
	2013 – 2022	54.3	24.24	86.18	9.64	37.33	21.92	10.1